Article

NS2B-D55E and NS2B-E65D Variations Are Responsible for Differences in NS2B-NS3 Protease Activities Between Japanese Encephalitis Virus Genotype I and III in Fluorogenic Peptide Model

Abdul Wahaab [1,2], Yan Zhang [1], Ke Liu [1], Jason L. Rasgon [2], Lei Kang [1], Muddassar Hameed [1], Chenxi Li [1], Muhammad Naveed Anwar [1], Yanbing Zhang [1], Anam Shoaib [3], Beibei Li [1], Yafeng Qiu [1], Jianchao Wei [1,*] and Zhiyong Ma [1,*]

[1] Shanghai Veterinary Research Institute, Chinese Academy of Agricultural Sciences, Shanghai 200241, China; wahaaabwahaaab@gmail.com (A.W.); 18672550235@163.com (Y.Z.); liuke@shvri.ac.cn (K.L.); kangshanglin1122@outlook.com (L.K.); muddassarh@vt.edu (M.H.); 007659@yzu.edu.cn (C.L.); dr.naveed903@gmail.com (M.N.A.); zhangyanbing@shzu.edu.cn (Y.Z.); lbb@shvri.ac.cn (B.L.); yafengq@shvri.ac.cn (Y.Q.)
[2] The Department of Entomology, Center for Infectious Disease Dynamics, and the Huck Institutes of the Life Sciences, Pennsylvania State University, University Park, PA 16802, USA; jlr54@psu.edu
[3] School of Behavioral and Brain Sciences, University of Texas at Dallas, Richardson, TX 75080, USA; anamshoaib45@gmail.com
* Correspondence: jianchaowei@shvri.ac.cn (J.W.); zhiyongma@shvri.ac.cn (Z.M.)

Abstract: Japanese encephalitis virus (JEV) NS2B-NS3 is a protein complex composed of NS3 proteases and an NS2B co-factor. The N-terminal protease domain (180 residues) of NS3 (NS3(pro)) interacts directly with a central 40-amino acid hydrophilic domain of NS2B (NS2B(H)) to form an active serine protease. In this study, the recombinant NS2B(H)-NS3(pro) proteases were prepared in *E. coli* and used to compare the enzymatic activity between genotype I (GI) and III (GIII) NS2B-NS3 proteases. The GI NS2B(H)-NS3(pro) was able to cleave the sites at the internal C, NS2A/NS2B, NS2B/NS3, and NS3/NS4A junctions that were identical to the sites proteolytically processed by GIII NS2B(H)-NS3(pro). Analysis of the enzymatic activity of recombinant NS2B(H)-NS3(pro) proteases using a model of fluorogenic peptide substrate revealed that the proteolytical processing activity of GIII NS2B(H)-NS3(pro) was significantly higher than that of GI NS2B(H)-NS3(pro). There were eight amino acid variations between GI and GIII NS2B(H)-NS3(pro), which may be responsible for the difference in enzymatic activities between GI and GIII proteases. Therefore, recombinant mutants were generated by exchanging the NS2B(H) and NS3(pro) domains between GI and GIII NS2B(H)-NS3(pro) and subjected to protease activity analysis. Substitution of NS2B(H) significantly altered the protease activities, as compared to the parental NS2B(H)-NS3(pro), suggesting that NS2B(H) played an essential role in the regulation of NS3(pro) protease activity. To further identify the amino acids responsible for the difference in protease activities, multiple substitution mutants including the individual and combined mutations at the variant residues 55 and 65 of NS2B(H) were generated and subjected to protease activity analysis. Replacement of NS2B-55 and NS2B-65 of GI to GIII significantly increased the enzymatic activity of GI NS2B(H)-NS3(pro) protease, whereas mutation of NS2B-55 and NS2B-65 of GIII to GI remarkably reduced the enzymatic activity of GIII NS2B(H)-NS3(pro) protease. Overall, these data demonstrated that NS2B-55 and NS2B-65 variations in the hydrophilic domain of NS2B co-contributed to the difference in NS2B(H)-NS3(pro) protease activities between GI and GIII. However, it will be crucial to explore these mutations in other in vivo and/or in vitro models. Collectively, these observations will be useful for understanding the replication of JEV GI and GIII viruses.

1. Introduction

Zika virus (ZIKV), Dengue virus (DENV), and Japanese encephalitis virus (JEV) are mosquito-borne members of the genus flavivirus and are resurging and emerging pathogens responsible for enormous disease burden. The flavivirus genome is ~11 kb single-stranded, positive-sense RNA comprising a large open reading frame encoding a single protein precursor, which is cleaved by a complex combination of cellular and viral-encoded proteases during and immediately after translation. This cleavage generates three structural [Capsid (C), precursor membrane (prM), Envelope (E)] and seven nonstructural (NS1, NS2, NS2b, NS3, NS4a, NS4b, and NS5) proteins necessary for viral genome replication [1–3]. JEV was first isolated in 1935 and since then has been classified into five genotypes (GI–GV) with geographic distribution in all continents except Antarctica, encompassing 67,900 human cases annually with a case fatality rate approaching 20–30%, with 30–50% of survivors suffering from neurological sequelae [4–7].

JEV GI emerged in the 1990s and has progressively replaced GIII as the most frequently isolated JEV genotype from stillborn piglets, *Culex tritaeniorhynchus* mosquitoes, and clinical JE patients in Korea, China, Vietnam, India, Thailand, Taiwan, and Japan [8–14]. It is suggested that JEV GI possibly competes with JEV GIII in the same pig–mosquito cycle and has a transmission advantage over areas formerly dominated by GIII [11,15]. Emerging JEV GI replicates more efficiently in wild birds, ducklings, and cell cultures derived from *Aedes albopictus* mosquitoes compared to GIII [16–20] and shows similar infectivity in *Culex pipiens* [21]; however, it is unclear if the replication efficiency of JEV GI vs. JEV GIII occurs in *Culex tritaeniorhynchus* mosquitoes and/or pigs, which have a crucial role in local JEV transmission. Additionally, experimental evidence linked with variance in viral genomic factors does not fully explain the occurrence of JEV GIII replacement during the past two decades [11,17,22].

JEV encodes a protease complex comprising the viral NS3 protein and an NS2B cofactor, which are requisite for generating functional viral particles. NS2B is an integral membrane protein comprising two hydrophobic and a central hydrophilic domain and plays a crucial role in viral replication [23,24]. The central hydrophilic region of NS2B(H) comprising around 50 residues is essential for the activation of NS3pro and accurate processing of viral polyprotein and is the principal determinant in substrate selection [25–27]. NS3 usually possesses RNA Helicase, serine proteases, RNA triphosphatase, and Nucleoside triphosphatase enzymatic activities [28]. These two-component-encoded NS2B-NS3 proteases are involved in polypeptide processing, RNA replication, and infectious particle assembly via enzymatic-independent or -dependent processes and thus substitutions may augment viral replications in different hosts [29–31]. Moreover, this two-component protein harbors diverse strategies to escape host innate immunity [22,32]. It has the potential to cleave interferon stimulators and surface receptors of tyrosine kinase. These interferon antagonistic abilities facilitate efficient viral replication, viral particle release, and neuro-invasion, which contribute to augmented virulence and high mortality in laboratory animals [33–36]. Furthermore, NS2B/NS3 proteases are highly conserved among various flaviviruses and JEV genotypes, making them an ideal therapeutic target for the development of multiple natural and synthetic broad-spectrum antiviral drugs [3,37,38].

In this study, we have investigated the contribution of NS2B/NS3 proteases for their possible role in the emergence of JEV GI over previously emerged GIII in vitro, using a fluorogenic peptide-based model. The methodology involved the cloning, expression, and purification of active and inactive JEV GI and GIII Ns2B(H)-NS3(pro) serine proteases and obtaining numerical/fluorescence data through fluorescence resonance energy transfer (FRET) modeling, using substrate sites suspected to be cleaved by viral serine

proteases. The involvement of mutations in NS2B(H) hydrophilic and NS3(pro) protease domains with different proteolytic processing activities of GI and GIII was also determined using recombinant proteins. The identified genetic determinants will be crucial for the selection of genes to monitor GI virus evolution, replication, and activities in natural transmission cycles.

2. Results

2.1. Amino Acid Variation in Cleavage Sites and Viral NS2B-NS3 Proteases

JEV polyprotein is cleaved to generate functional proteins by a combination of host and viral proteases. The cleavage is anticipated to occur at connections between C/prM, prM/E, E/NS1, NS1/NS2A, NS2B/NS3, NS3/NS4A, NS4A/NS4B, and NS4B/NS5 and the sites of internal C, NS4A, and NS3 (Figure 1A). Alignment of prophesied cleavage site sequence revealed no variations among strains of GI and GIII (Figure 1B). However, the two-component viral NS2N(H)/NS3(pro) proteases involved in the proteolytic processing of virus polyprotein exhibited eight mutations between GI and III (Figure 1C). Two conserved mutations were spotted in the hydrophilic domain of NS2B region, i.e., E55D and D65E, with a conservation rate of 90–100%, and six mutations were spotted in the protease domain of the NS3 region, i.e., L14S, S78A, P105A, D177E, and K185R, with a conservation rate of 90–100% and S182N with a conservation rate of 58–89% (data obtained after alignment of 50 random represented strains from GI and GIII) [39]. Three mutations in the NS2B-NS3 regions of JEV were previously reported to be involved in the replication advantage of GI over GIII in avian cells at elevated temperatures [31]. However, the mechanism behind that advantage still needs to be investigated, making NS2B/NS3 a promising region to monitor virus evolution and genotype displacement.
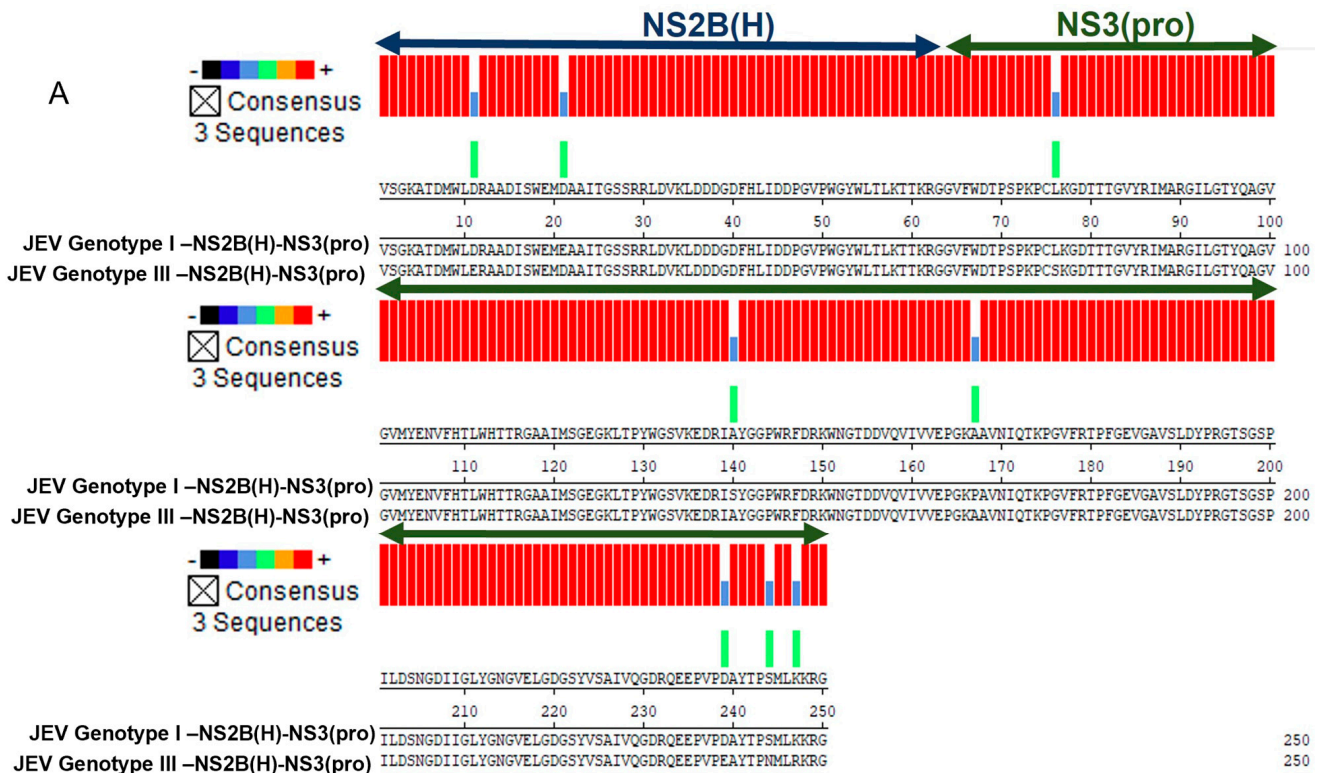

Figure 1. *Cont.*

B

NS2B
NS2A
NS4A
prM
NS4B

| C | | E | NS1 | | | NS3 | | | NS4B | NS5 |

Internal C
C/prM
prM/E
E/NS1
NS1/NS2A
NS2A/NS2B
NS2B/NS3
Internal NS3
NS3/NS4A
Internal NS4A
NS4A/NS4B
NS4B/NS5

Sites Cleaved by JEV Genotype III NS2B(H)-NS3(pro)

C

Cleavage site

------P4-P3-P2-P1 ↓ P1'- P2'- P3'- P4'------

Substrate sequence susceptible to proteases

C/prM
GI   LAIVTACAGA↓MKLSNFQGKL
GIII LAVVIACAGA↓MKLSNFQGKL

prM/E
ILLLLVAPAYS↓FNCLGMGNRD
ILLLLVAPAYS↓FNCLGMGNRD

E/NS1
VLVFLATNVHA↓DTGCAIDITR
VLVFLATNVHA↓DTGCAIDITR

NS1/NS2A
GI   TTLVRSQVDA↓FNGEMIDPFQ
GIII TTLVRSQVDA↓FNGEMVDPFQ

NS2A/NS2B
LMVCNPNKKR↓GWPATEFLSA
LMVCNPNKKR↓GWPATEFLSA

NS2B/NS3
YWLTLKTTKR↓GGVFWDTPSP
YWLTLKTTKR↓GGVFWDTPSP

NS3/NS4A
GI   WFKDFAAGKR↓SAVSFIEVLG
GIII WFKDFAAGKR↓SAVSFIEVLG

NS4A/NS4B
VLTVVGVVAA↓NEYGMLEKTK
VLTVVGVVAA↓NEYGMLEKTK

NS4B/NS5
KNADKPSLKR↓GRPGGRTLGE
KNADKPSLKR↓GRPGGRTLGE

internal C
GI   NKRGKKQNKR↓GGNESLIMWL
GIII NKRGRKQNKR↓GGNEGSIMWL

internal NS3
ITSASAAQRR↓GRVGRNPNQV
ITSASAAQRR↓GRVGRNPNQV

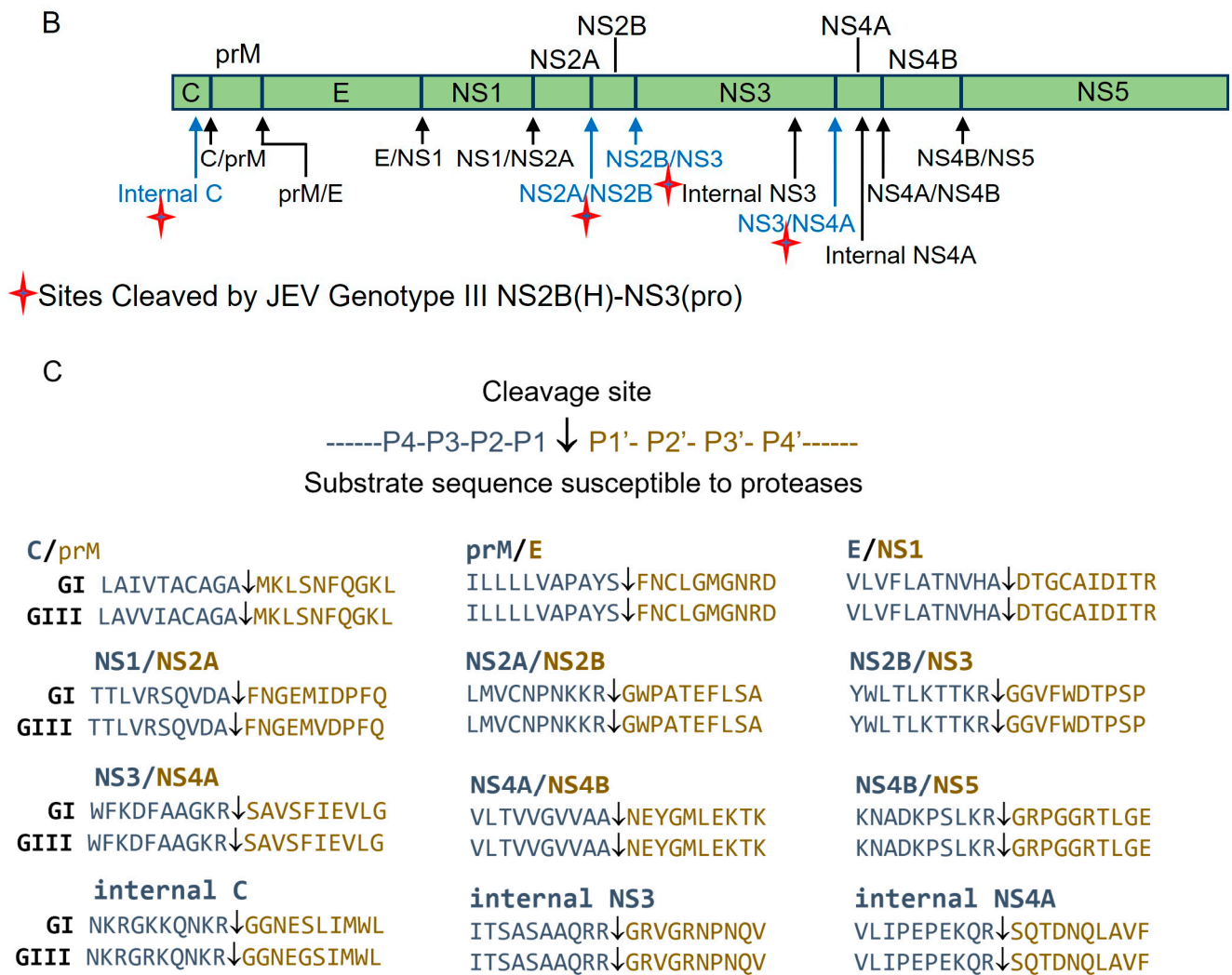internal NS4A
VLIPEPEKQR↓SQTDNQLAVF
VLIPEPEKQR↓SQTDNQLAVF

Figure 1. Japanese encephalitis virus two-component NS2B(H)/NS3(pro) proteases and cleavage sites predicted to be proteolytically processed by them. (**A**) Schematic diagram of JEV polyprotein with the predicted cleavage sites. Black arrowheads indicate the predicted cleavage sites and blue arrowheads represent the sites previously reported to be cleaved by JEV genotype III proteases (Wahaab et al., 2021). (**B**) Sequence alignment of the predicted cleavage sites for JEV genotypes I and III. Arrowheads indicate the predicted cleavage sites. (**C**) Sequence alignment of two-component JEV NS2B(H)/NS3(pro) proteases for JEV genotype I (SH7) and genotype III (SH15) showed eight amino acid substitutions between them, which are shaded in blue. Homologous amino acids are shaded in red color.

2.2. JEV GI and GIII NS2B(H)/NS3(pro) Proteases Exhibit Identical Cleavage Patterns for Proteolytic Processing of JEV Polyprotein

Studies have demonstrated that JEV protease activity mainly depends on the association between NS3 and its co-factor NS2B and that these two-component NS2B-NS3 proteases expressed in *E. coli* are folded correctly with effective proteolytic activity [28,40]. Therefore, in our previous study, we selected the prokaryotic cell model of *E. coli* to identify cleavage sites proteolytically processed by two-component JEV GIII-SH15 proteases [41]. GI-SH7, which exhibits different 3D protein conformations (Figure 7B) and eight critical substitutions (Figure 1C) in the protease region compared to GIII-SH15, was engineered to

a dual protein prokaryotic expression plasmid pETDuet-1 (Figure 2A) to observe and compare the cleavage pattern of artificial GFP substrate containing a cleavage site from GI-SH7 (Figure 2). The artificial GFP substrate, when expressed alone in *E. coli*, did not show any cleavage by *E. coli* proteases. When recombinant viral NS2B(H)-NS3(pro) was co-expressed with all artificial substrates individually, a 21 kDa band corresponding to the N-terminal part of the cleaved substrate was seen (Figure 2B). The identified cleavage sites were validated by the co-expression of all artificial substrate sites with inactivated/dead viral NS2B(H)-NS3(pro), which was generated by the substitution of serine at position 135 located in the catalytic trait of NS3 with alanine (Figure 2C). Cleavage of artificial GFP substrates was determined by Western blot using antibodies specific to GFP and the expressions of viral proteases were determined by anti-NS3. Here, our results demonstrated that GI-SH7 was able to cleave the sites at the internal C, NS2A/NS2B, NS2B/NS3, and NS3/NS4A junctions and exhibited the same cleavage pattern as previously reported for SH-GIII [41], suggesting that viral protease substitution and protein conformation do not interfere with the selection of cleavage sites for proteolytic processing and possibly play no role in genotype displacement. The blots are added as (Supplementary Figure S1).
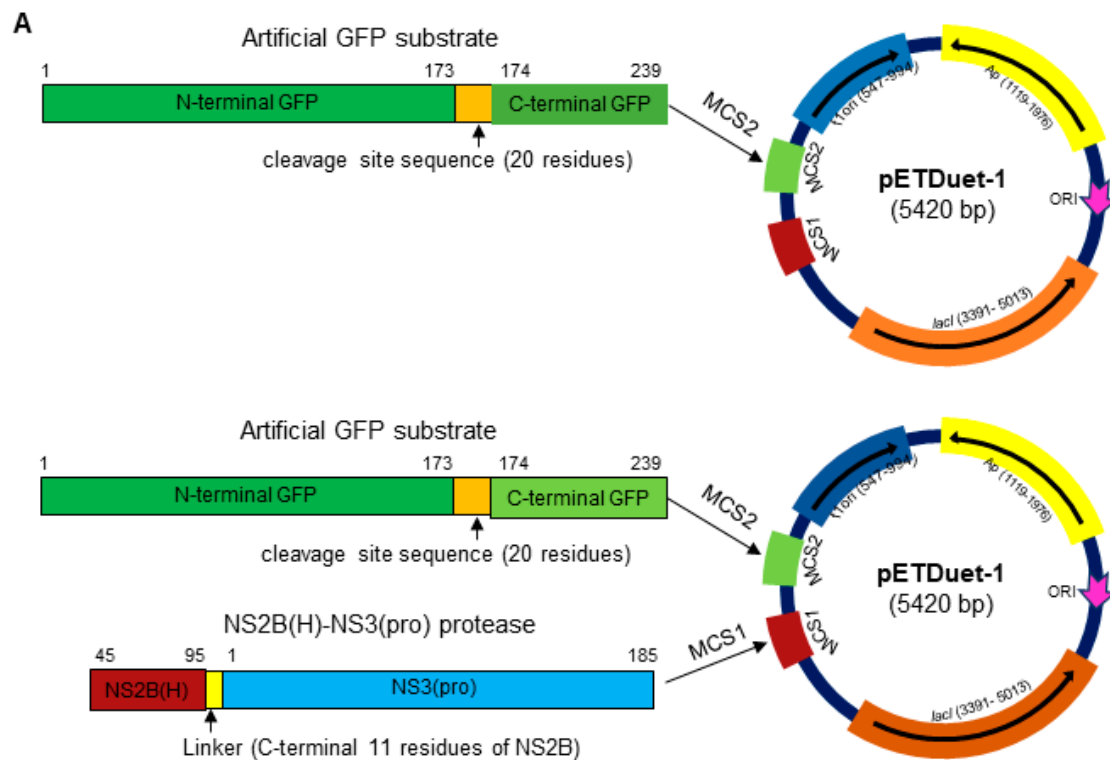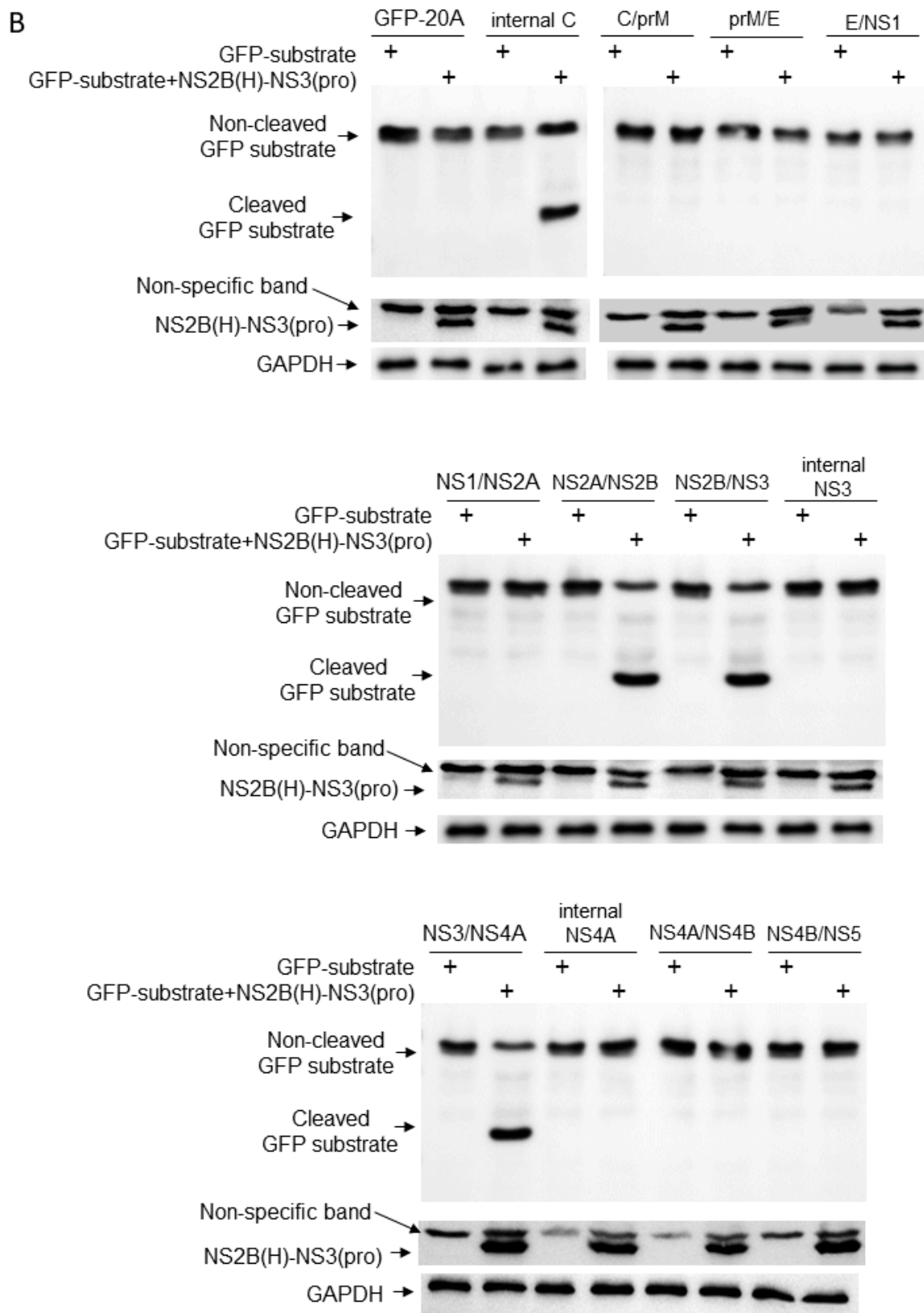

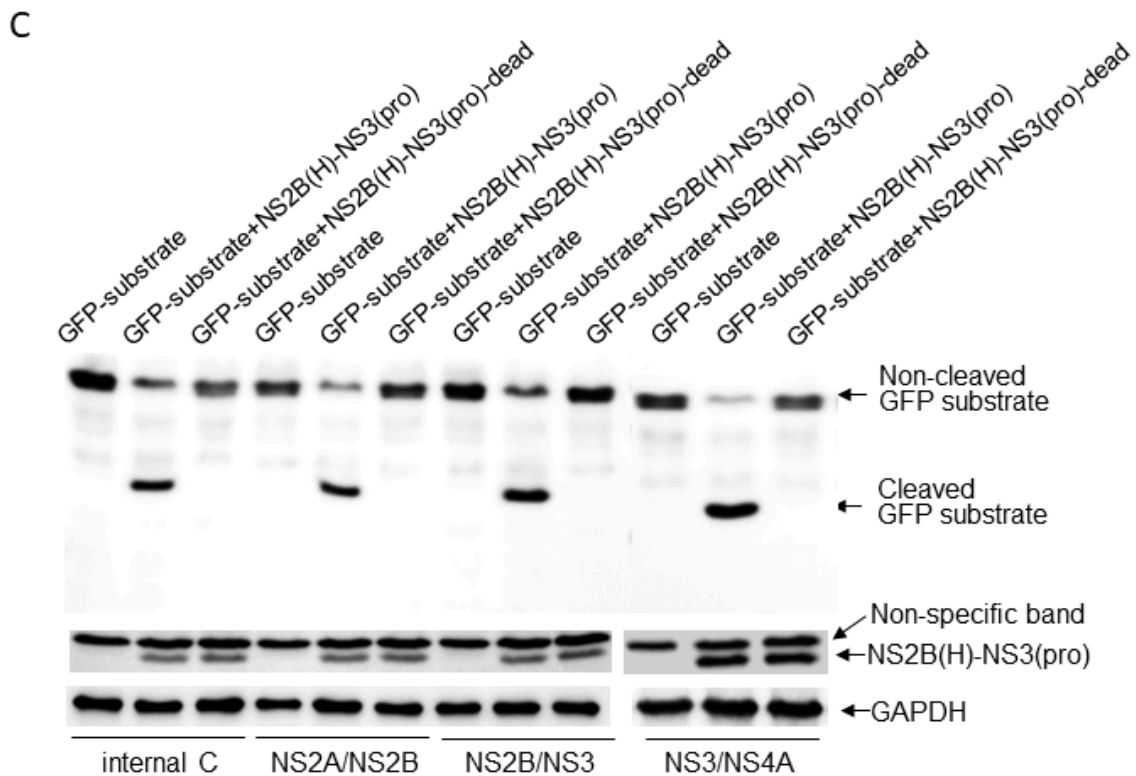**Figure 2.** *Cont.*

Figure 2. *Cont.*

Figure 2. Detection of cleavage sites by JEV genotype I NS2B(H)-NS3(pro) protease in *E. coli*. (**A**) Schematic representation of recombinant plasmids. (**B**) *E. coli* cells were transformed with recombinant plasmid dually expressing and artificial GFP substrate or with recombinant plasmid expressing artificial GFP substrate alone. Cleavage of the artificial GFP substrate in *E. coli* was examined by Western blot with antibodies specific to GFP. Expression of intact (non-cleaved) NS2B(H)-NS3(pro) protease was detected with antibodies specific to NS3. (**C**) Identified cleavage sites were validated by transforming *E. coli* cells with recombinant plasmid dually expressing active NS2B(H)-NS3(pro) protease and artificial GFP substrate (GFP-substrate + NS2B(H)-NS3(pro)), or inactive NS2B(H)-NS3(pro) protease and artificial GFP substrate (GFP-substrate + NS2B(H)-NS3(pro)-dead), or with recombinant plasmid expressing artificial GFP substrate alone. Cleavage of artificial GFP substrates in *E. coli* was examined by Western blot with antibodies specific to GFP. Expression of intact (non-cleaved) NS2B(H)-NS3(pro) protease was detected with antibodies specific to NS3.

2.3. Preparation of Recombinant NS2B(H)-NS3(pro) Proteases

Studies have demonstrated that JEV protease activity mainly depends on the association between NS3 and its co-factor NS2B and that this two-component NS2B-NS3 protease expressed in *E. coli* is folded correctly with effective proteolytic activity [28,40]. To analyze and compare the proteolytic processing activities of GI-SH7 and GIII-SH15 NS2B/NS3 proteases, the active and inactivated NS2B(H)-NS3(pro) proteases were structured and engineered into P-TrcHisA vectors for expression in *E. coli* (Figure 3A). SDS-PAGE and Western immunoblotting of purified proteins was performed with antibodies specific to polyhistidine and JEV-NS3. SDS-PAGE revealed the presence of three bands. The intact band of viral NS2B(H)-NS3(pro) proteases was seen at 36 kDa, whereas the autocleavage bands of NS3(pro) and NS2B(H) [40] were observed at 21 kDa and 10 kDa, respectively, for each active SH7 and SH15 protease (Figure 3B). However, only the intact NS2B(H)-NS3(pro) at 36 KDa was seen for inactivated/dead NS2B/NS3 proteases of both strains (Figure 3B), confirming its inactivity. The SDS-PAGE blots were quantified using ImageJ software (imageJ 1.54g) to determine the self-cleavage percentage of NS2B-NS3 proteases of both strains. SH7 was self-cleaved with a rate of 77.5% and SH15 with a rate of 99.1%. The purified NS2B(H)-NS3(pro) proteases were further confirmed by Western blot with antibodies specific to His-tag and NS3, respectively. Distinct differences in intact anti-His

and anti-NS3 expression were also seen between both strains (Figure 3C). Overall, these observations suggest that GIII-SH15 shows a high autocleavage rate of enzymatically active NS2B(H)-NS3(pro) proteases compared to GI-SH7. However, no autocleavage was seen for the dead/inactivated viral proteases of both strains.
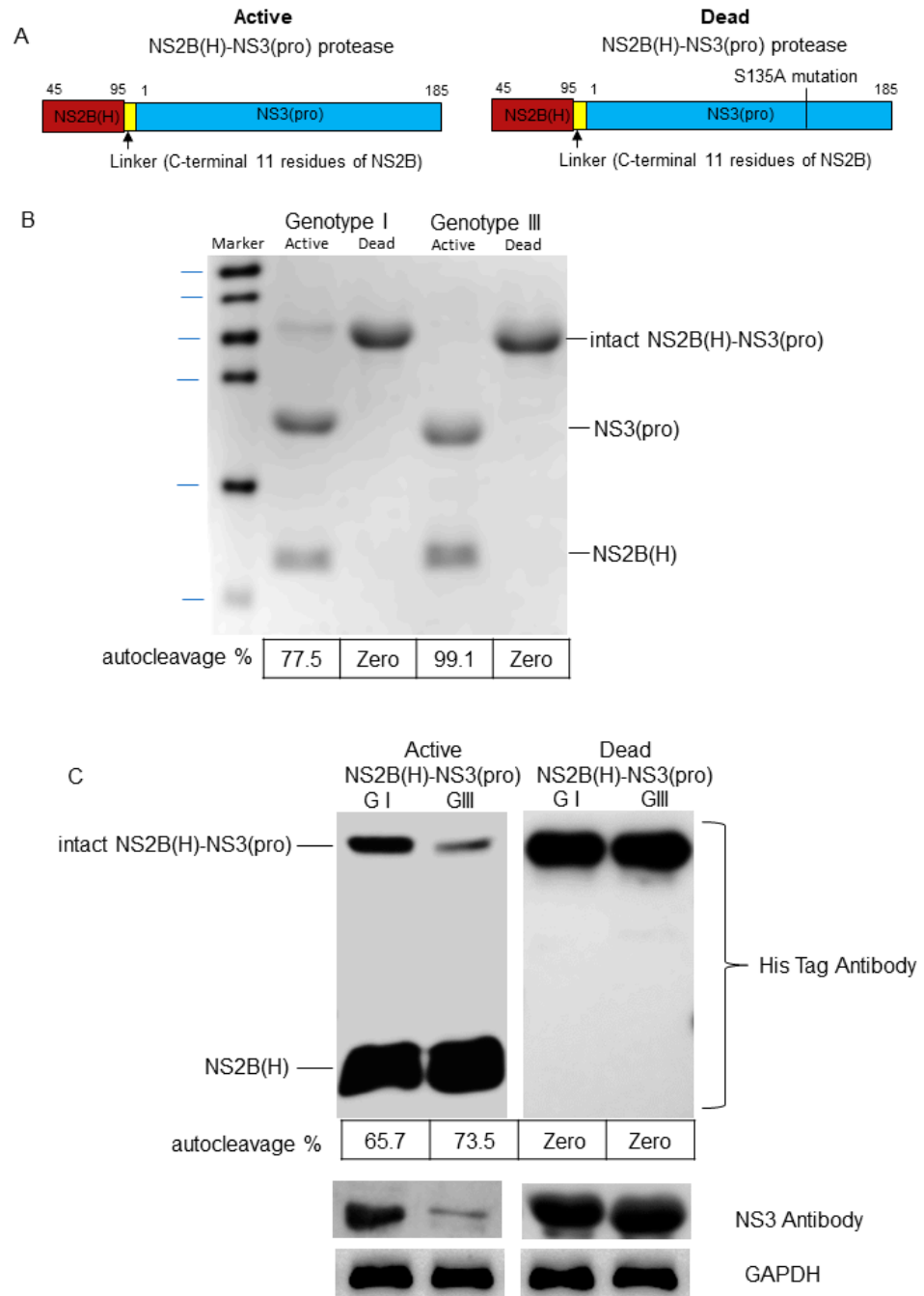

Figure 3. Cloning, expression, and purification of active and dead recombinant NS2B(H)-NS3(pro) proteases. (**A**) Schematic representation of recombinant plasmids. (**B**) SDS-PAGE for active and dead proteases NS2B(H)-NS3pro of GI and GIII. (**C**) Western blot was performed for active and dead NS2B(H)-NS3 of GI and GIII using His tag, JEV NS3, and GADBH antibodies. The bands were quantified by ImageJ software to determine the self-cleavage percentage.

2.4. Analysis of Proteolytic Processing Activities of GI and GIII NS2B(H)-NS3(pro) Proteases Using Fluorogenic Model

The enzymatic activity of GI-SH7 and GIII-SH15 recombinant NS2B(H)-NS3(pro) proteases was examined and compared by fluorescence obtained after the hydrolysis of fluorogenic peptide substrates containing the sequence identical to the dibasic cleavage sites of NS2A/NS2B and NS2B/NS3 from JEV polyprotein [40,42]. The assays conducted to compare the proteolytic activities of active and inactivated proteases using the fluorogenic peptide containing the cleavage site sequence from JEV NS2B-NS3 revealed that all four groups of proteases did not display any significant differences in florescence at zero minutes, indicating the non-hydrolysis of the suspectable cleavage site at a specific time point. However, after a twenty-minute interval, a statistically significant difference was seen between GI-SH7 and GIII-SH15 (Figure 4A). The GI-SH7 and GIII-SH15 also exhibited statistical differences from their respective dead proteases, indicating cleavage of the fluorogenic substrate by the active proteases of both strains. The fluorescence value kept increasing with the passage of time and the values became constant at 480 min. Significant differences were observed at all time points between GI-SH7 and GIII-SH15 from twenty minutes and onwards. The dead protease fluorescence data remained constant without any increase after zero minutes throughout the experiment (Figure 4A).

The experiments were repeated using synthetic fluorogenic peptides from the cleavage sites of JEV NS2A/NS2B. All four groups of proteases did not display any difference in fluorescence data at zero minutes. At twenty minutes, a statistically significant difference was seen between GI-SH7 and GIII-SH15 (Figure 4B). The GI-SH7 and GIII-SH15 proteases also exhibited statistically significant differences from their respective dead/inactive proteases. These kinetic values kept increasing and became constant at 480 min. The dead proteases' fluorescence data remained constant without any increase throughout the experiment, indicating the non-hydrolysis of the fluorogenic substrate by dead proteases (Figure 4B). Collectively, these findings revealed that proteases from GIII-SH15 possess high proteolytic processing activities compared to GI-SH7, and the artificial fluorogenic peptides containing cleavage sites from NS2B/NS3 are more efficiently cleaved by JEV proteases compared to site NS2A/NS2B.
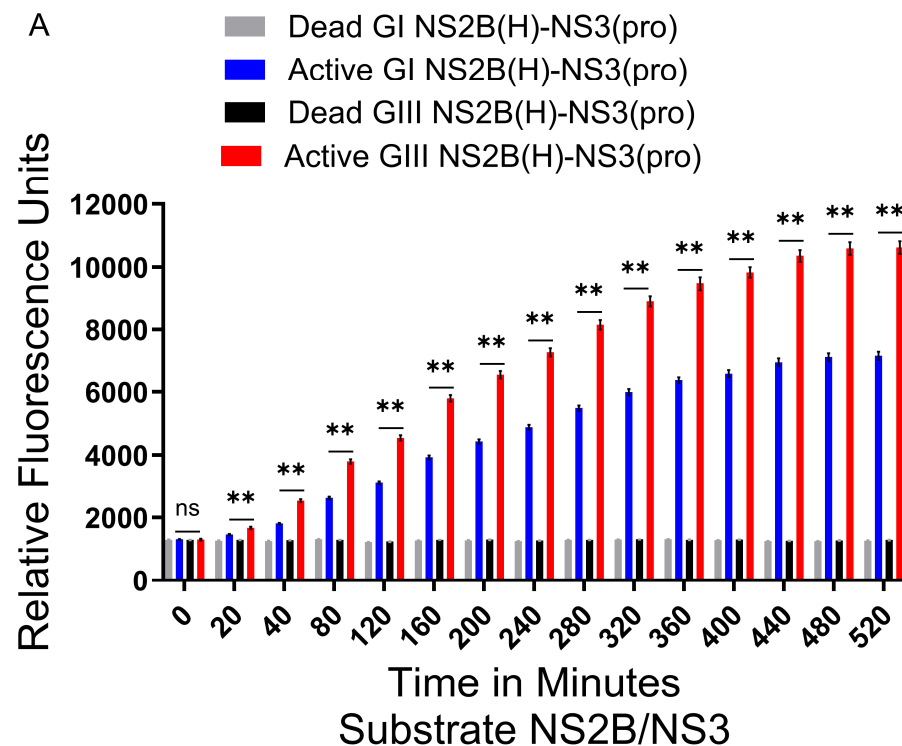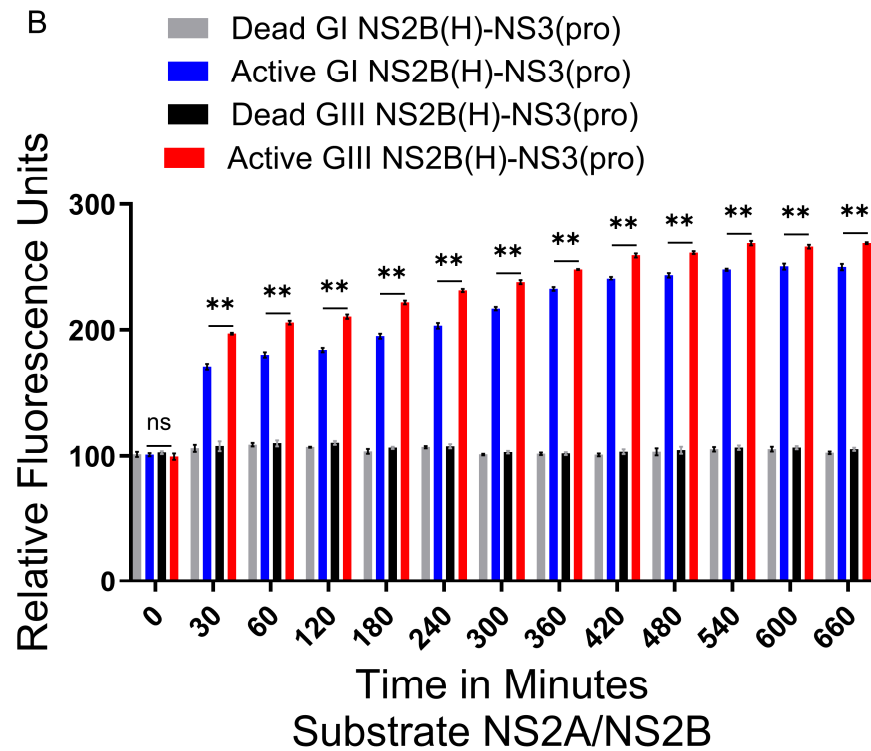

Figure 4. *Cont.*

Figure 4. Active and dead JEV NS2B(H)-NS3(pro) catalyzed substrate hydrolysis rates. (**A**) The graph shows fluorescence/relative enzyme activities' difference in active and dead JEV genotype I and III NS2B(H)-NS3(pro) proteases for hydrolysis/cleavage of Pyr-RTKR-AMC, a substrate site obtained from JEV cleavage site NS2B-NS3. A non-significant ($p > 0.05$) difference was seen at zero minutes ($p = 0.9372$). A statistically significant ($p \leq 0.01$) difference with consistent p value ($p = 0.0022$) was seen from 20 min time point until 520 min when active GI-SH7 NS2B(H)-NS3(pro) was compared with active GIII-SH15 NS2B(H)-NS3(pro) proteases. (**B**) The graph represents fluorescence/relative enzyme activities' difference in JEV genotype I and III active and dead NS2B(H)-NS3(pro) proteases for hydrolysis/cleavage of Dabcyl-PNKKRGWPAT-(Edans)G, a substrate cleavage site obtained from JEV NS2A-NS2B. A non-significant ($p > 0.05$) difference was seen at zero minutes ($p = 0.8182$). A statistically significant ($p \leq 0.01$) difference with consistent p value ($p = 0.0022$) was seen from 30 min time point until 660 min when active GI-SH7 NS2B(H)-NS3(pro) was compared with active GIII-SH15 NS2B(H)-NS3(pro) proteases. Statistical differences are presented as follows: ns (non-significant), $p > 0.05$; and **, $p \leq 0.01$.

2.5. Proteolytic Processing Activities of GI and GIII NS2B(H)-NS3(pro) Proteases at Elevated Temperatures

The higher thermal stability at elevated temperatures for GI could be a causative factor related to the enhancement in viral replication of GI viruses. Previously, NS2B/NS3 mutations in JEV were found to enhance the infectivity of GI over GIII in amplifying host cells at elevated temperatures [31]. To assess the influence of viral thermal stability on viral NS2B/NS3 protease proteolytic activities, the experiment was repeated using elevated temperatures of 41 °C with fluorogenic substrate NS2B/NS3. All viral proteases did not display any hydrolysis of fluorogenic peptide at zero minutes. From twenty minutes onwards, a statistically significant difference was seen between GI-SH7 and GIII-SH15 activities (Figure 4A). These fluorescence values kept increasing variably (maintaining the significant difference between both genotypes) and became constant at 400 min onwards, while the dead protease fluorescence data remained constant without any increase throughout the experiment (Figure 5). These results were similar to experiments performed at 37 °C (Figure 4) and indicated that elevated temperatures do not influence the proteolytic processing activities of viral proteases.
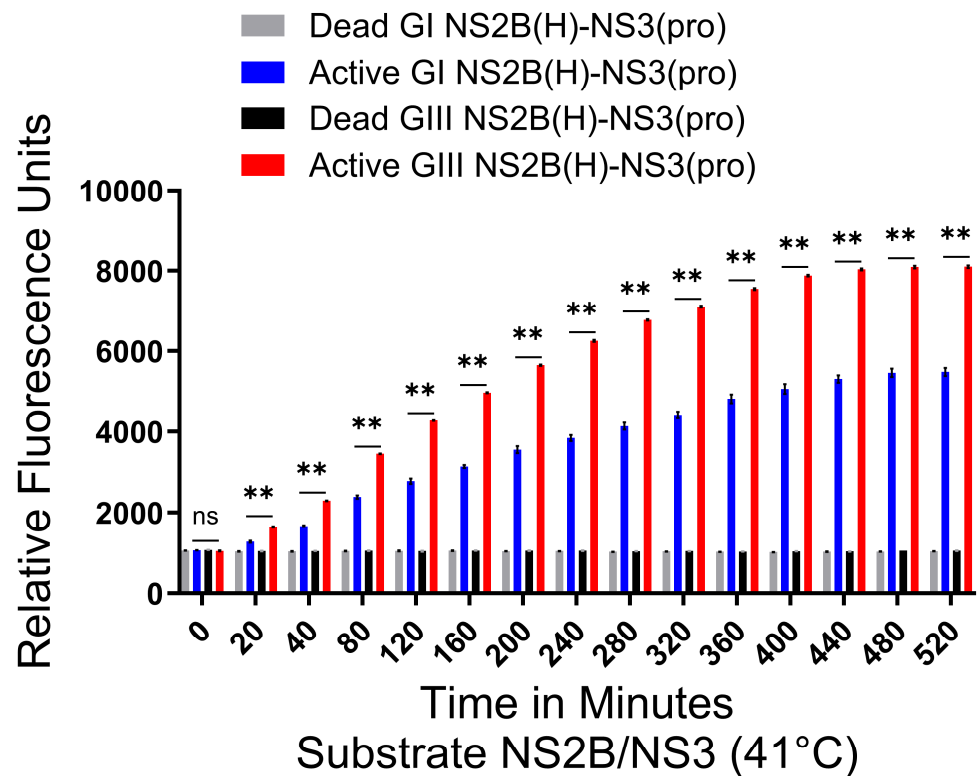
Figure 5. Active and dead JEV NS2B(H)-NS3(pro) catalyzed substrate hydrolysis rates at elevated temperatures. The graph represents fluorescence/relative enzyme activities' difference in JEV genotype I and III active and dead NS2B(H)-NS3(pro) proteases for hydrolysis/cleavage of Pyr-RTKR-AMC, a substrate site obtained from JEV NS2B-NS3 at elevated temperatures, i.e., 41 °C. A non-significant ($p > 0.05$) difference was seen at zero minutes ($p = 0.1797$) between all groups. A statistically significant ($p \leq 0.01$) difference with consistent p value ($p = 0.0022$) was seen from 20 min time point until 520 min when active GI-SH7 NS2B(H)-NS3(pro) was compared with active GIII-SH15 NS2B(H)-NS3(pro) proteases. Statistical differences are presented as follows: ns (non-significant), $p > 0.05$; and **, $p \leq 0.01$.

2.6. Hydrophilic Domain of NS2B Determines the Difference in NS2B(H)-NS3(pro) Protease Activities Between GI and GIII

As a synthetic fluorogenic peptide harboring a cleavage site from NS2B/NS3 was cleaved more efficiently by JEV proteases, it was selected to determine whether hydrophilic amino acid variations in the protease domain in viral proteases are involved in increased proteolytic processing or the hydrolysis of fluorogenic peptides of GIII-SH15 over GI-SH7. Recombinant proteases were generated by exchanging proteins encoding the hydrophilic domain from NS2B and protease domain from NS3 of the respective GI-SH7 and GIII-SH15 strains, resulting in GI/NS2B(H)-GIII/NS3(pro) and GIII/NS2B(H)-GI/NS3(pro) (Figure 6A). Exchanging the hydrophilic domain of GI NS2B to GIII in GI protease (GIII/NS2B(H)-GI/NS3(pro)) significantly increased its proteolytic processing activities as compared with the parental GI NS2B(H)-NS3(pro) protease (Figure 6B). The activity of GIII/NS2B(H)-GI/NS3(pro) became almost similar to that of GIII NS2B(H)-NS3(pro) with no significant difference among them (Figure 6C).
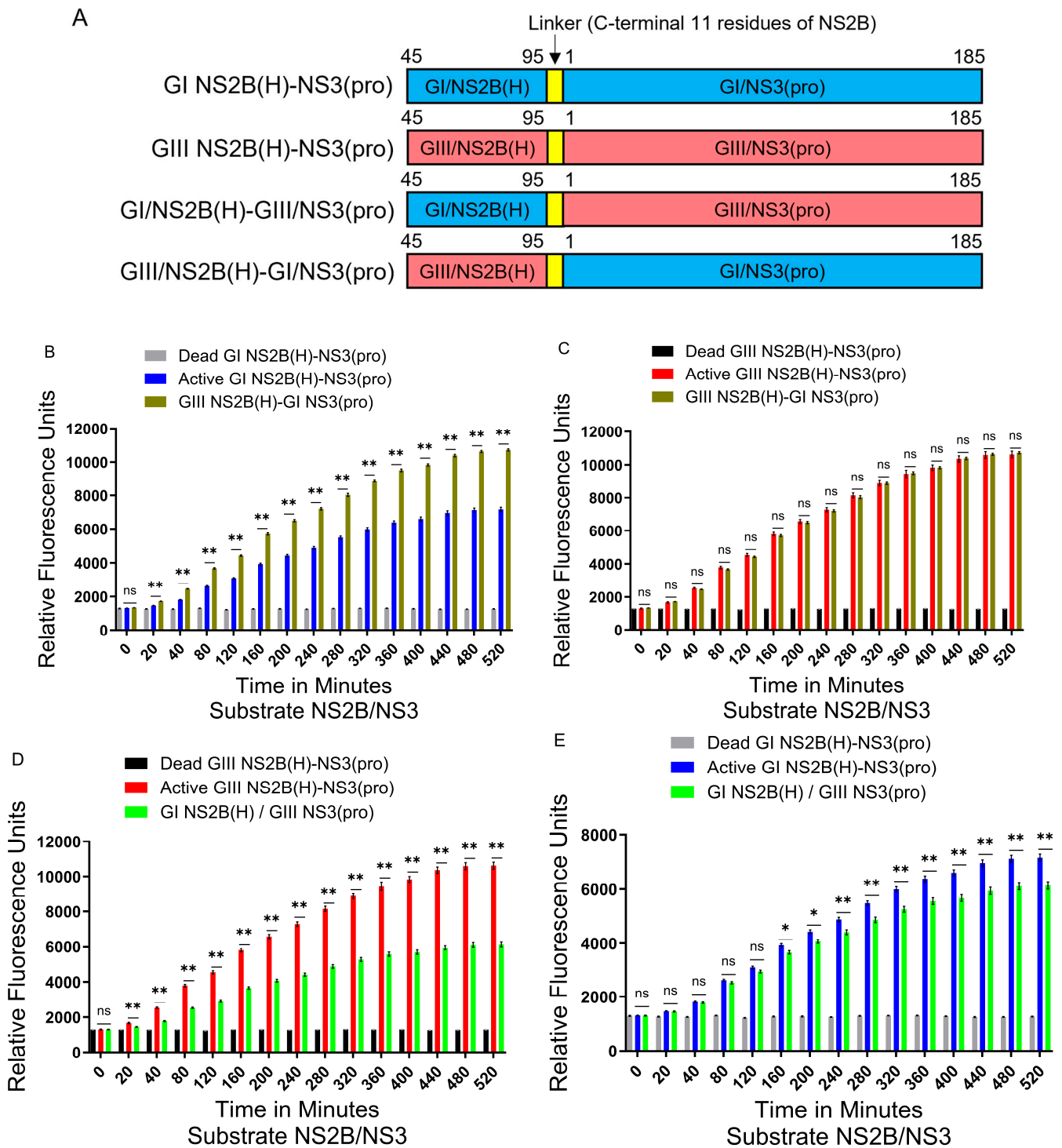
Figure 6. Role of NS2B hydrophilic domain in differential hydrolysis rates/proteolytic processing activities: (**A**) Schematic representation of reversed JEV GI-SH7, i.e., GIII NS2B(H)-GI NS3(pro) with exchanged hydrophilic domain from GIII-SH15 and reversed JEV GIII-SH15, i.e., GI NS2B(H)/GIII NS3(pro) with exchanged hydrophilic domains from GI-SH7. (**B,C**) The graphs represent and compare fluorescence/relative enzyme activities' difference in JEV genotype GI-SH7 (**B**) and GIII-SH15 (**C**) with reversed JEV GI-SH7, i.e., GIII NS2B(H)-GI NS3(pro) for hydrolysis/cleavage of Pyr-RTKR-AMC, a substrate site obtained from JEV NS2B-NS3. (**B**) A non-significant ($p > 0.05$) difference was seen at zero minutes ($p = 0.0931$). A statistically significant ($p \leq 0.01$) difference with a consistent p value ($p = 0.0022$) was seen from the 20 min time point until 520 min when compared with GI-SH7 NS2B(H)-NS3(pro). (**C**) Similarly, a non-significant ($p > 0.05$) difference was seen from zero minutes

(p = 0.4848) time point until 520 min (p = 0.8182) with variable p values at different time points when compared with GIII-SH15 NS2B(H)-NS3(pro) proteases. (**D,E**) The graphs represent and compare fluorescence/relative enzyme activities' difference in JEV genotype GIII-SH15 (**D**) and GI-SH7 (**E**) with reversed JEV GIII-SH15, i.e., GI NS2B(H)-GIII NS3(pro) for hydrolysis/cleavage of Pyr-RTKR-AMC, a substrate site obtained from JEV NS2B-NS3. (**D**) A non-significant (p > 0.05) difference was seen at zero minutes (p = 0.0932). A statistically significant ($p \leq 0.01$) difference with consistent p value (p = 0.0022) was seen from the 20 min time point until 520 min when compared with GIII-SH15 NS2B(H)-NS3(pro) proteases. (**E**) Similarly, a non-significant (p > 0.05) difference was seen at zero minutes (p = 0.8182), 20 min (p = 0.6991), 40 min (p = 0.4848), 80 min (p = 0.2043), and 120 min (p = 0.0649). A statistically significant difference ($p \leq 0.05$) was seen at 160 min (p = 0.0260) and 200 min (p = 0.0152), followed by a highly statistically significant ($p \leq 0.01$) difference at 240 min (p = 0.0087). From 280 until 520 min, a highly significant ($p \leq 0.01$) difference with consistent p value (p = 0.0043) was observed when compared with GI-SH7 NS2B(H)-NS3(pro) proteases. Statistical differences are presented as follows: ns (non-significant), p > 0.05; *, $p \leq 0.05$; and **, $p \leq 0.01$.

After exchanging the hydrophilic domain of GIII NS2B to GI in GIII proteases (GI/NS2B(H)-GIII/NS3(pro)), a significant decrease in the activity of GI/NS2B(H)-GIII/NS3(pro) protease was observed compared to the parental GIII NS2B(H)-NS3(pro) protease (Figure 6D). The levels of GI/NS2B(H)-GIII/NS3(pro) protease activity were similar to those of the GI NS2B(H)-NS3(pro) protease during 20 to 120 min, but significantly lower than those of the GI NS2B(H)-NS3(pro) protease from 160 min (Figure 6E). Collectively, these results demonstrate that the hydrophilic domain of NS2B determined the difference in NS2B(H)-NS3(pro) protease activities between GI and GIII, suggesting that the mutations in the hydrophilic domain of NS2B may be responsible for the difference in NS2B(H)-NS3(pro) protease activities between GI and GIII.

2.7. Contribution of NS2B-D55E Variation in Hydrophilic Domain of NS2B to the Difference in NS2B(H)-NS3(pro) Protease Activities Between GI and GIII

The hydrophilic domain of NS2B is responsible for differences in proteolytic processing activities between GI and GIII NS2B(H)-NS3(pro) proteases. This specific domain possesses two variations at positions 55 (NS2B-D55E) and 65 (NS2B-E65D) in the NS2B protein (Figure 1C). Data obtained after alignment of fifty represented strains of GI and GIII revealed that both mutations have a conservation rate of 90–100% [39]. To determine the contribution of NS2B-D55E to differential proteolytic processing activities between GI and GIII NS2B(H)-NS3(pro) proteases, we replaced aspartic acid (D) at position 55 of the GI NS2B(H)-NS3(pro) protease with glutamic acid (E) to generate a mutant protease of GI NS2B(H)/D55E-NS3(pro) and substituted aspartic acid (D) for glutamic acid (E) at position 55 of GIII NS2B(H)-NS3(pro) protease to generate a mutant protease of GIII NS2B(H)/E55D-NS3(pro) (Figure 7A). The substitution of NS2B-D55E variation resulted in a conformational change in NS2B(H), as compared with its respective parent (Figure 7B). The mutants of GI NS2B(H)/D55E-NS3(pro) and GIII NS2B(H)/E55D-NS3(pro) were prepared, and their proteolytic processing activities compared with their parental GI NS2B(H)-NS3(pro) and GIII NS2B(H)-NS3(pro) proteases. Exchanging the amino acid residue at 55 in GI NS2B(H) from aspartic acid to glutamic acid significantly increased the proteolytic processing activities of GI NS2B(H)/D55E-NS3(pro), as compared to its parental GI NS2B(H)-NS3(pro) protease (Figure 7C). However, the levels of GI NS2B(H)/D55E-NS3(pro) protease activities remained significantly lower than those of GIII NS2B(H)-NS3(pro) protease from 40 min and onwards (Figure 7D). These results indicate that the substitution of NS2B-D55E contributed to the increased proteolytic processing of GI NS2B(H)/D55E-NS3(pro) over its parental GI NS2B(H)-NS3(pro). When the amino acid at position 55 in GIII NS2B(H) was exchanged from glutamic acid to aspartic acid, the levels of GIII NS2B(H)/E55D-NS3(pro) protease activities significantly decreased, as compared to its parental GIII NS2B(H)-NS3(pro) protease (Figure 7E) but remained higher than those of GI NS2B(H)-NS3(pro) protease (Figure 7F). Collectively, these results demonstrated that

the NS2B-D55E variation in the hydrophilic domain of NS2B contributed to the difference in NS2B(H)-NS3(pro) protease activities between GI and GIII.
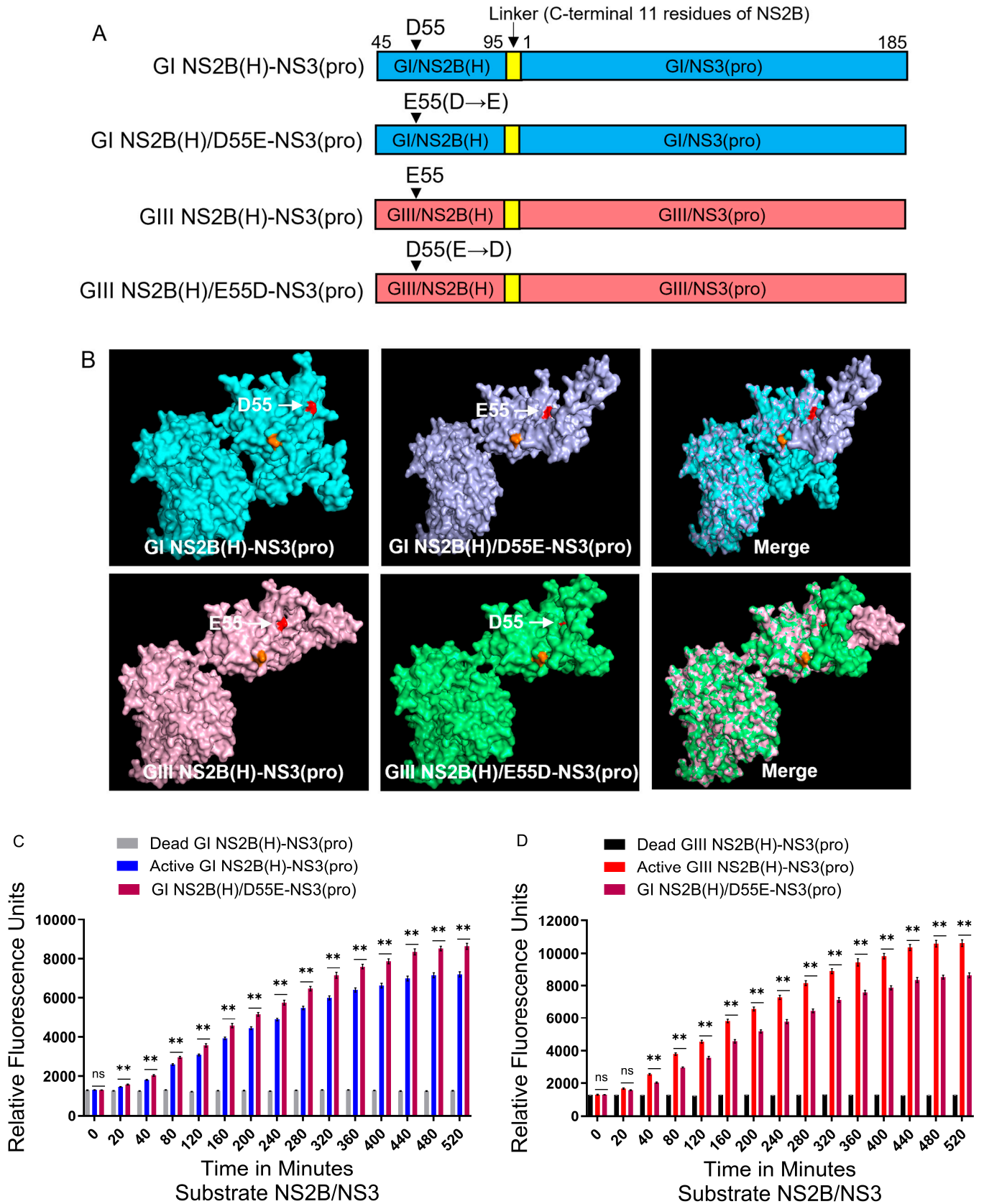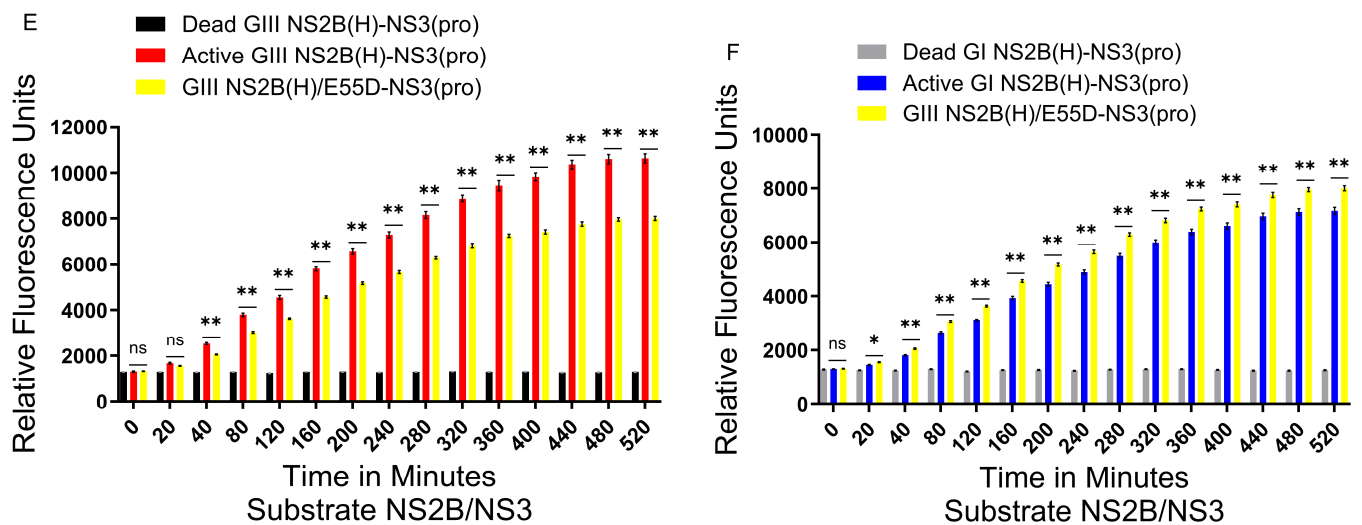

Figure 7. *Cont.*

Figure 7. Contribution of variation 55 in the hydrophilic domain of NS2B to proteolytic activities of NS2B(H)-NS3(pro). (**A**). Schematic diagram of reversed JEV GI-SH7, i.e., GI NS2B(H)/D55E-NS3(pro) and reversed JEV GIII-SH15 i.e., GIII NS2B(H)/E55D-NS3(pro) with exchanged NS2B-55 variations from their respective parent NS2B(H)-NS3(pro) proteases. (**B**) The graph represents and compares 3D structural conformations of reversed JEV GI-SH7, i.e., GI-SH7, i.e., GI NS2B(H)/D55E-NS3(pro) and reversed JEV GIII-SH15, i.e., GIII NS2B(H)/E55D-NS3(pro) with their respective parent GI-SH7 and GIII-SH15 NS2B(H)-NS3(pro) proteases. Variation NS2B(H)55 is highlighted in red. (**C,D**) The graphs represent and compare reaction velocities/relative enzyme activities' difference in JEV genotype GI-SH7 (**C**) and GIII-SH15 NS2B(H)-NS3(pro) proteases (**D**) with reversed JEV GI-SH7, i.e., GI NS2B(H)/D55E-NS3(pro) for hydrolysis/cleavage of Pyr-RTKR-AMC, a substrate site obtained from JEV NS2B-NS3. (**C**) A non-significant ($p > 0.05$) difference was seen at zero minutes time point ($p = 0.8182$). A statistically significant ($p \leq 0.01$) difference was seen at 20 min ($p = 0.0043$) time point and consistent statistically significant ($p = 0.0022$) difference was seen from the 40 min time point until 520 min when compared with GI-SH7 NS2B(H)-NS3(pro) proteases. (**D**) Similarly, a non-significant ($p > 0.05$) difference was seen for zero ($p = 0.5887$) and 20 min ($p = 0.0649$) time points. A statistically significant ($p \leq 0.01$) difference with consistent p value ($p = 0.0022$) was seen from the 40 min time point until 520 min when it was compared with GIII-SH15 NS2B(H)-NS3(pro) proteases. (**E,F**) The graphs represent and compare reaction velocities/relative enzyme activities' difference in JEV genotype GI-SH7 (**F**) and GIII-SH15 (**E**) NS2B(H)-NS3(pro) proteases with reversed JEV GIII-SH15, i.e., GIII NS2B(H)/E55D-NS3(pro) for hydrolysis/cleavage of Pyr-RTKR-AMC, a substrate site obtained from JEV NS2B-NS3. (**E**) A non-significant ($p > 0.05$) difference was seen for zero ($p = 0.9372$) and 20 min ($p = 0.0649$) time points. A statistically significant ($p \leq 0.01$) difference with consistent p value ($p = 0.0022$) was seen from the 40 min time point until 520 min when it was compared with GIII-SH15 NS2B(H)-NS3(pro) proteases. (**F**) Similarly, a non-significant ($p > 0.05$) difference was seen at zero minutes ($p = 0.3939$). A statistically significant ($p \leq 0.05$) difference was seen at the 20 min time point ($p = 0.0152$), followed by a highly significant ($p \leq 0.01$) difference with consistent p value ($p = 0.0022$) seen from 40 until 520 min when compared with GI-SH7 NS2B(H)-NS3(pro) proteases. Statistical differences are presented as follows: ns (non-significant), $p > 0.05$; *, $p \leq 0.05$; and **, $p \leq 0.01$.

2.8. Contribution of NS2B-E65D Variation in Hydrophilic Domain of NS2B to the Difference in NS2B(H)-NS3(pro) Protease Activities Between GI and GIII

To determine the contribution of NS2B-E65D variation in the hydrophilic domain of NS2B to the difference in NS2B(H)-NS3(pro) protease activities between GI and GIII, we replaced glutamic acid (E) at position 65 of GI NS2B(H)-NS3(pro) protease with aspartic acid (D) to generate a mutant protease of GI NS2B(H)/E65D-NS3(pro) and substituted glutamic acid (E) for aspartic acid (D) at position 65 of GIII NS2B(H)-NS3(pro) protease to generate a mutant protease of GIII NS2B(H)/D65E-NS3(pro) (Figure 8A). The substitution of NS2B-E65D variation resulted in a conformational change in NS2B(H), as compared

with its respective parent (Figure 8B). The mutants of GI NS2B(H)/E65D-NS3(pro) and GIII NS2B(H)/D65E-NS3(pro) were prepared, and their proteolytic processing activities were compared with their parental GI NS2B(H)-NS3(pro) and GIII NS2B(H)-NS3(pro) proteases. Exchanging the amino acid residue at position 65 in GI NS2B(H) from glutamic acid to aspartic acid significantly increased the proteolytic processing activities of GI NS2B(H)/E65D-NS3(pro), as compared to its parental GI NS2B(H)-NS3(pro) protease (Figure 8C). However, the levels of GI NS2B(H)/E65D-NS3(pro) protease activities remained lower than those of GIII NS2B(H)-NS3(pro) protease (Figure 8D). These results indicated that the co-substitution of NS2B-E65D contributed to the increased proteolytic processing of GI NS2B(H)/E65D-NS3(pro) over its parental GI NS2B(H)-NS3(pro). When the amino acid residue at position 65 in GIII NS2B(H) was exchanged from aspartic acid to glutamic acid, the levels of GIII NS2B(H)/D65E-NS3(pro) protease activities significantly decreased, as compared to its parental GIII NS2B(H)-NS3(pro) protease (Figure 8E) but remained higher than those of GI NS2B(H)-NS3(pro) protease (Figure 8F). Collectively, these results demonstrated that the NS2B-E65D variation in the hydrophilic domain of NS2B contributed to the difference in NS2B(H)-NS3(pro) protease activities between GI and GIII.
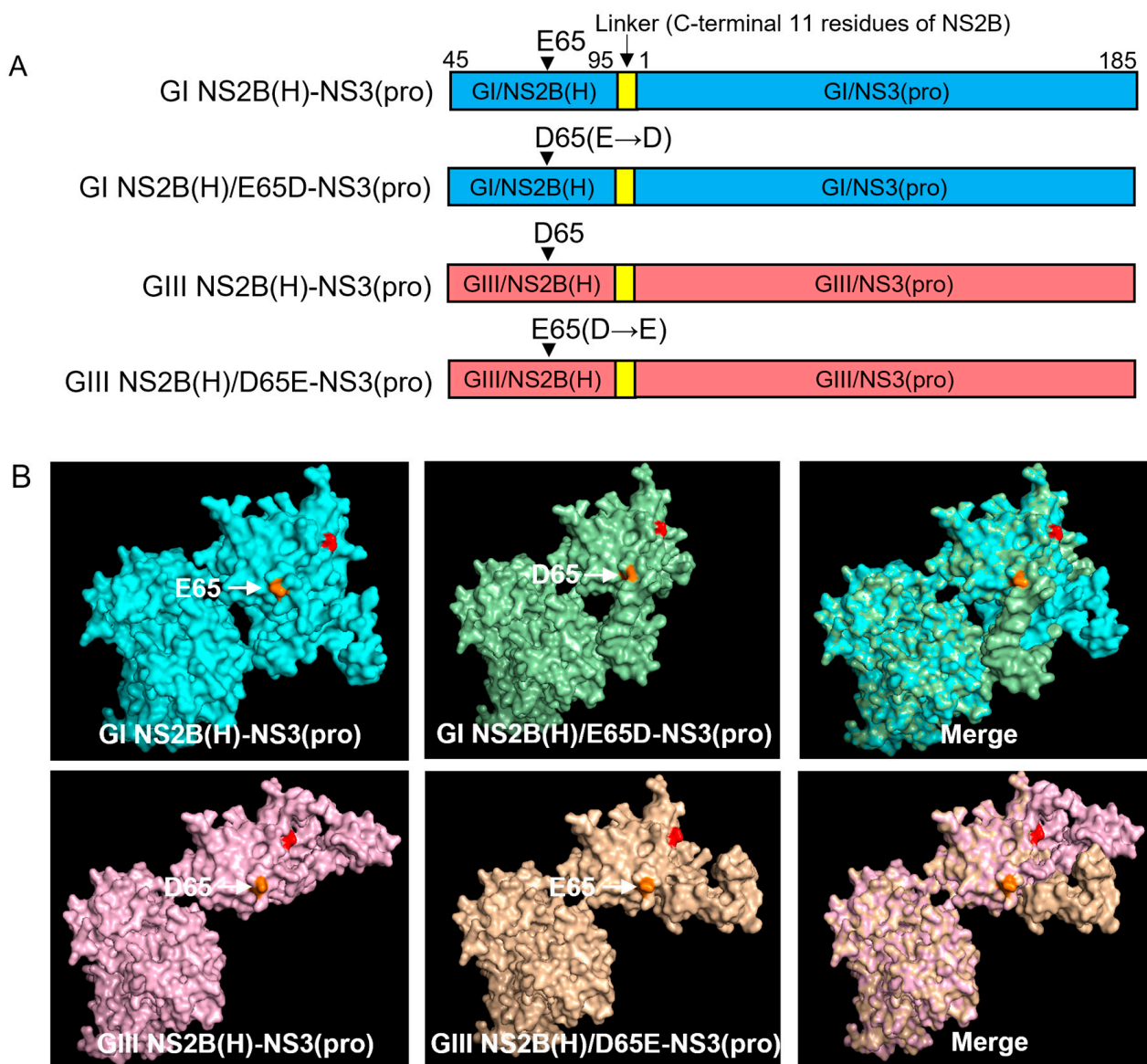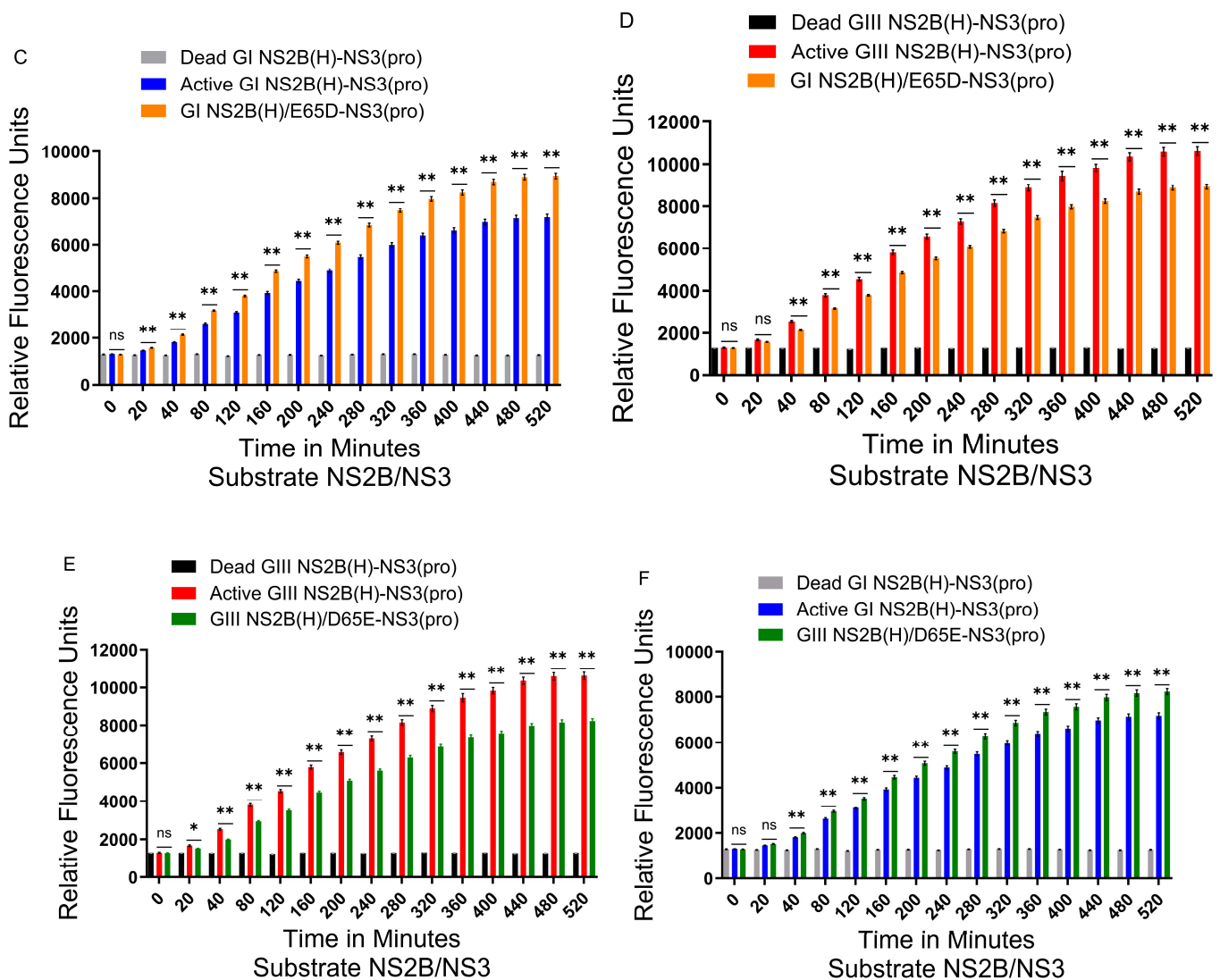

Figure 8. *Cont.*

Figure 8. Contribution of variation 65 in the hydrophilic domain of NS2B to proteolytic activities of NS2B(H)-NS3(pro). (**A**) Schematic diagram of reversed JEV GI-SH7, i.e., GI NS2B(H)/E65D-NS3(pro) and reversed JEV GIII-SH15, i.e., GIII NS2B(H)/D65E-NS3(pro) with exchanged NS2B-65 variations from their respective parent NS2B(H)-NS3(pro) proteases. (**B**) The graph represents and compares 3D structural conformations of reversed JEV GI-SH7, i.e., GI NS2B(H)/ E65D-NS3(pro) and reversed JEV GIII-SH15, i.e., GIII NS2B(H)/D65E-NS3(pro) with their respective parent GI-SH7 and GIII-SH15 NS2B(H)-NS3(pro) proteases. Variation NS2B(H)65 is highlighted in yellow. (**C,D**) The graphs represent and compare fluorescence/relative enzyme activities' difference in JEV genotype GI-SH7 (**C**) and GIII-SH15 NS2B(H)-NS3(pro) proteases (**D**) with reversed JEV GI-SH7, i.e., GI NS2B(H)/E65D-NS3(pro) for hydrolysis/cleavage of Pyr-RTKR-AMC, a substrate site obtained from JEV NS2B-NS3. (**C**) A non-significant ($p > 0.05$) difference was seen at zero minutes ($p = 0.4848$). A significant ($p \leq 0.01$) difference with a consistent p value ($p = 0.0022$) was seen from the 20 min time point until 520 min when compared with GI-SH7 NS2B(H)-NS3(pro) proteases. (**D**) Similarly, a non-significant ($p > 0.05$) difference was seen for zero ($p = 0.6991$) and 20 min ($p = 0.1797$). A significant ($p \leq 0.01$) difference with a consistent p value ($p = 0.0022$) was seen from the 20 min time point until 520 min when compared with GIII-SH15 NS2B(H)-NS3(pro) proteases. (**E,F**) The graphs represent and compare fluorescence/relative enzyme activities' difference in JEV genotype GI-SH7 (**F**) and GIII-SH15 (**E**) NS2B(H)-NS3(pro) proteases with reversed JEV GIII-SH15, i.e., GIII NS2B(H)/D65E-NS3(pro) for hydrolysis/cleavage of Pyr-RTKR-AMC, a substrate site obtained from JEV NS2B-NS3. (**E**) A non-significant ($p > 0.05$) difference was seen at zero minutes ($p = 0.5887$).

A statistically significant ($p \leq 0.05$) difference was seen at the 20 min time point ($p = 0.0152$), followed by a highly significant ($p \leq 0.01$) difference with consistent p value ($p = 0.0022$) seen from 40 until 520 min when compared with GIII-SH15 NS2B(H)-NS3(pro) proteases. (**F**) Similarly, a non-significant ($p > 0.05$) difference was seen for zero ($p = 0.2403$) and 20 min ($p = 0.0649$) time points. A statistically significant ($p \leq 0.01$) difference with consistent p value ($p = 0.0022$) was seen from the 40 min time point until 520 min when compared with GI-SH7 NS2B(H)-NS3(pro) proteases. Statistical differences are presented as follows: ns (non-significant), $p > 0.05$; *, $p \leq 0.05$; and **, $p \leq 0.01$.

2.9. Co-Contribution of NS2B-D55E and NS2B-E65D Variations in Hydrophilic Domain of NS2B to the Difference in NS2B(H)-NS3(pro) Protease Activities Between GI and GIII

Variation in the hydrophilic domain of both NS2B-D55E and NS2B-E65D contributed individually to the difference in NS2B(H)-NS3(pro) protease activities between GI and GIII. The amino acid residues at positions 55 and 65 of NS2B were simultaneously exchanged between GI and GIII NS2B(H)-NS3(pro) proteases to generate the co-substitution mutants of GI NS2B(H)/D55E/E65D-NS3(pro) and GIII NS2B(H)/E55D/D65E-NS3(pro) (Figure 9A). Co-substitution of NS2B-D55E and NS2B-E65D resulted in a conformational change in NS2B(H), as compared with its respective parent (Figure 9B). Analysis of the proteolytic processing activity indicated that co-substitution of NS2B-D55E and NS2B-E65D significantly increased the levels of the proteolytic processing activity of GI NS2B(H)/D55E/E65D-NS3(pro), as compared to those of its parental GI NS2B(H)-NS3(pro) (Figure 9C); the levels increased by co-substitution were similar to those of GIII NS2B(H)-NS3(pro) (Figure 9D). Together, these results indicated that co-substitution of NS2B-D55E and NS2B-E65D contributed collectively to the increased proteolytic processing of GI NS2B(H)/D55E/E65D-NS3(pro) over its parental GI NS2B(H)-NS3(pro). On the other hand, the co-substitution of NS2B-E55D and NS2B-D65E altered the proteolytic processing activity of GIII NS2B(H)-NS3(pro). The levels of proteolytic processing activity of GIII NS2B(H)/E55D/D65E-NS3(pro) were significantly lower than those of its parental GIII NS2B(H)-NS3(pro) (Figure 9E) as well as relatively lower than those of GI NS2B(H)-NS3(pro) (Figure 9F). Overall, these data suggested that NS2B-D55E and NS2B-E65D variations in the hydrophilic domain of NS2B co-contributed to the difference in NS2B(H)-NS3(pro) protease activities between GI and GIII. However, additional studies on the structural basis of JEV NS2B-NS3 proteins should be conducted to elucidate conformational changes caused by these variants in detail. It will also be crucial to employ a glycosylated vector model system to investigate the interaction between these mutations and viral glycosylation, specifically in relation to the role of JEV NS2B-NS3 proteases in genotype shift. Lastly, the GI and GIII possess six mutations (i.e., L14S, S78A, P105A, D177E, S182N, and K185R) in the NS3-pro region. Exploring these mutations individually and different combinations could provide deeper insight into their role in differential protease activities and genotype shifts.
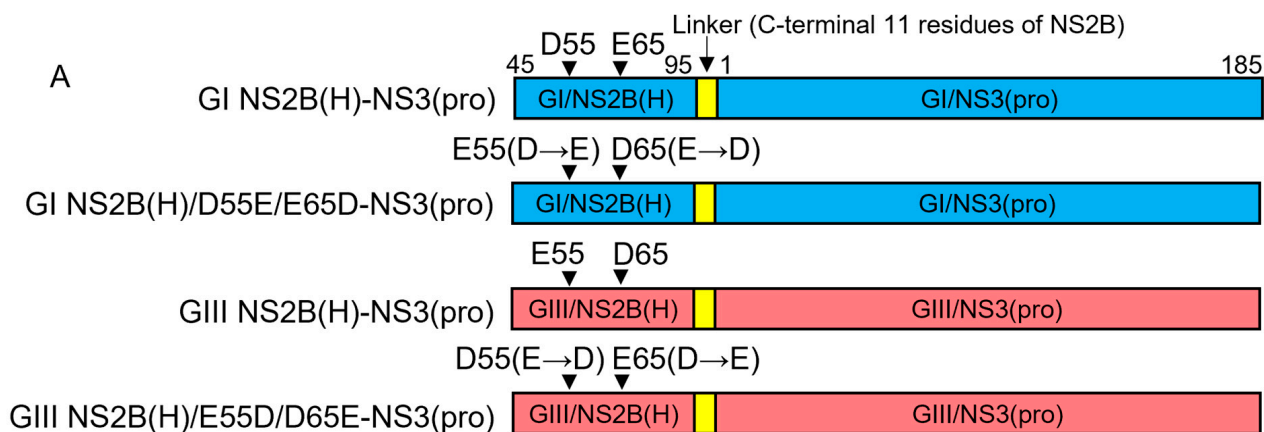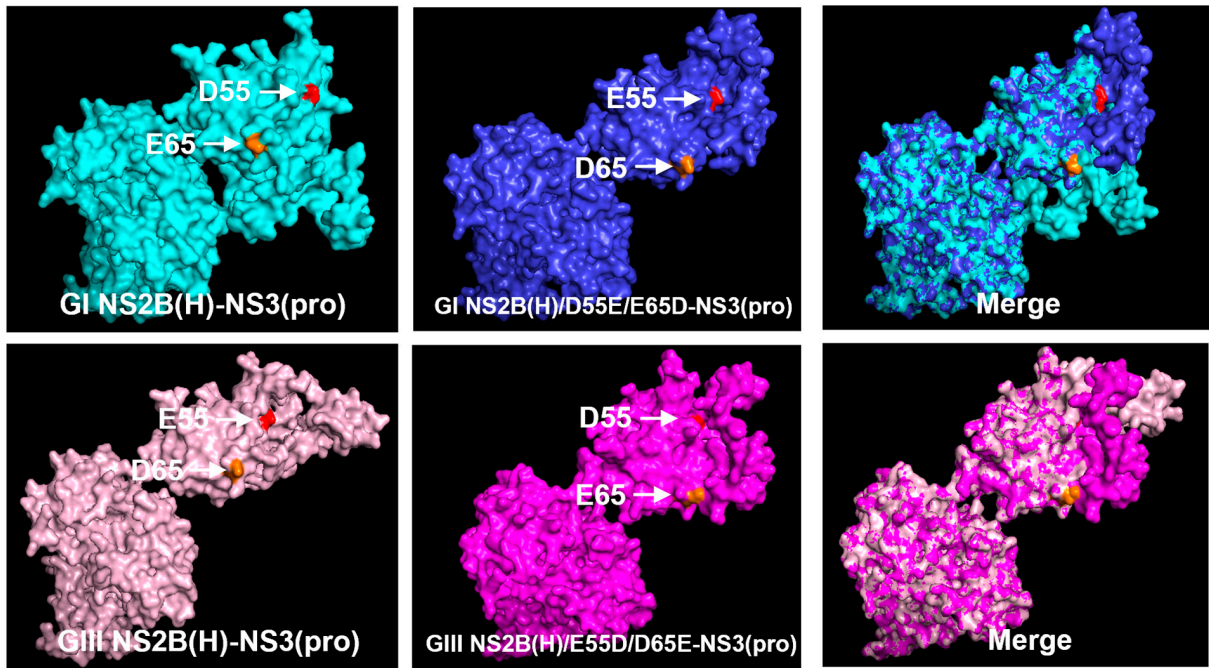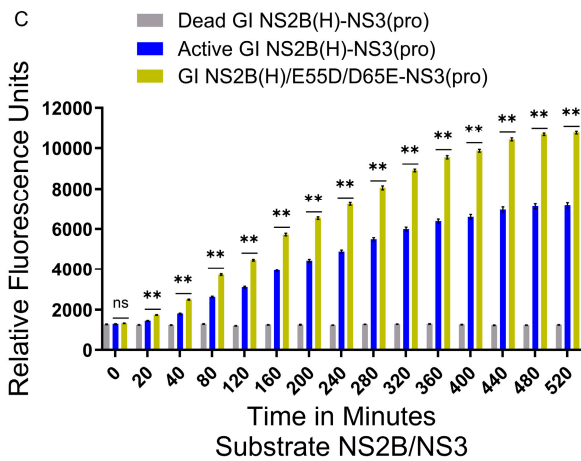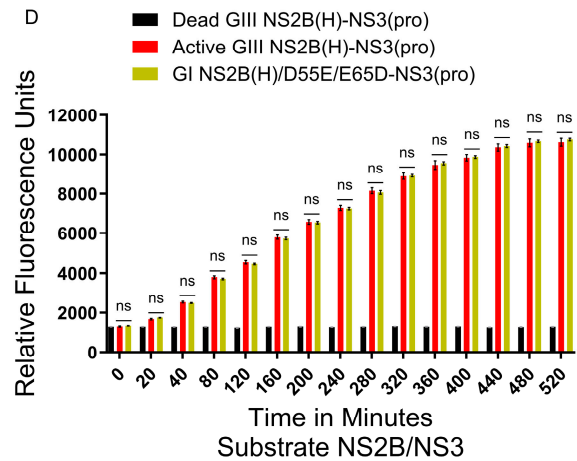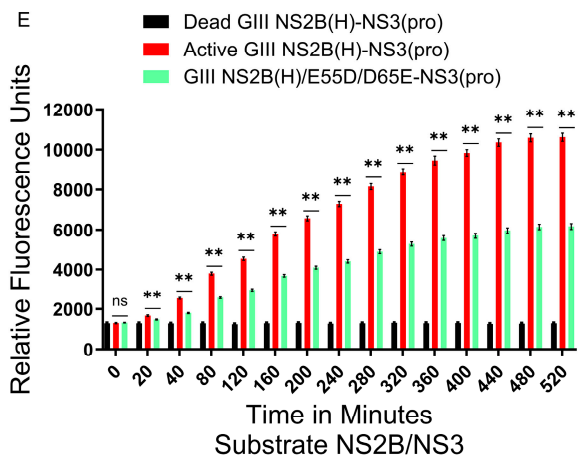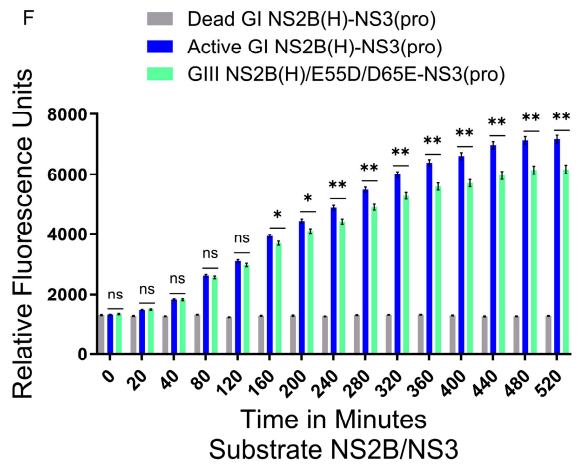

Figure 9. *Cont.*

Figure 9. Co-contribution of NS2B-D55E and NS2B-E65D variations in the hydrophilic domain of NS2B to proteolytic activities of NS2B(H)-NS3(pro). (**A**) Schematic diagram of reversed JEV GI-SH7,

i.e., GI NS2B(H)/D55E/E65D-NS3(pro) and reversed JEV GIII-SH15, i.e., GIII NS2B(H)/E55D/D65E-NS3(pro) with exchanged NS2B-D55E and NS2B-E65D variations from their respective parent NS2B(H)-NS3(pro) proteases. (**B**) The graph represents and compares 3D structural conformations of reversed JEV GI-SH7, i.e., GI NS2B(H)/D55E/E65D-NS3(pro) and reversed JEV GIII-SH15, i.e., GIII NS2B(H)/E55D/D65E-NS3(pro) with their respective parent GI-SH7 and GIII-SH15 NS2B(H)-NS3(pro) proteases. Variations NS2B(H)55 and NS2B(H) 65 are highlighted in red and yellow, respectively. (**C**,**D**) The graphs represent and compare fluorescence/relative enzyme activities' difference in JEV genotype GI-SH7 (**C**) and GIII-SH15 NS2B(H)-NS3(pro) proteases (**D**) with reversed JEV GI-SH7, i.e., GI NS2B(H)/D55E/E65D-NS3(pro) for hydrolysis/cleavage of Pyr-RTKR-AMC, a substrate site obtained from JEV NS2B-NS3. (**C**) A non-significant ($p > 0.05$) difference was seen at zero minutes. A statistically significant ($p \leq 0.01$) difference with a consistent p value was seen from the 20 min time point until 520 min when compared with GI-SH7 NS2B(H)-NS3(pro) proteases. (**D**) Similarly, a non-significant ($p > 0.05$) difference was seen from zero minutes time point until 520 min ($p = 0.8182$) with variable p values at different time points when compared with GIII-SH15 NS2B(H)-NS3(pro) proteases. (**E**,**F**) The graphs represent and compare fluorescence/relative enzyme activities' difference in JEV genotype GI-SH7 (**F**) and GIII-SH15 (**E**) NS2B(H)-NS3(pro) proteases with reversed JEV GIII-SH15, i.e., GIII NS2B(H)/E55D/D65E-NS3(pro) for hydrolysis/cleavage of Pyr-RTKR-AMC, a substrate site obtained from JEV NS2B-NS3. (**E**) A non-significant ($p > 0.05$) difference was seen at zero minutes. A statistically significant ($p \leq 0.01$) difference with consistent p value ($p = 0.0022$) was seen from the 20 min time point until 520 min when compared with GIII-SH15 NS2B(H)-NS3(pro) proteases. (**F**) Similarly, a non-significant ($p > 0.05$) difference was seen at zero minutes, 20 min, 40 min, 80 min, and 120 min. A statistically significant difference ($p \leq 0.05$) was seen at 160 min ($p = 0.0260$) and 200 min ($p = 0.0152$), followed by a highly significant ($p \leq 0.01$) difference at 240 min ($p = 0.0087$). From 280 until 520 min, a highly significant ($p \leq 0.01$) difference with consistent p value ($p = 0.0043$) was observed when compared with GI-SH7 NS2B(H)-NS3(pro)proteases. Statistical differences are presented as follows: ns (non-significant), $p > 0.05$; *, and $p \leq 0.05$; **.

3. Discussion

The emerging JEV GI virus has gradually displaced the JEV GIII virus as a dominant virus genotype isolated from stillborn piglets, *Culex tritaeniorhynchus*, and human cases since the 1990s. The mechanism behind this genotype replacement remains unclear. In this study, we have identified the contribution of JEV NS2B(H)-NS3(pro) protease determinants, which are correlated with the enhanced proteolytic processing activities of GIII proteases using the fluorogenic peptide substrate model.

JEV polyprotein is cleaved to generate functional proteins by a complex combination of host and viral proteases. The cleavage is predicted to occur at junctions between C/prM, prM/E, E/NS1, NS1/NS2A, NS2B/NS3, NS3/NS4A, NS4A/NS4B, and NS4B/NS5 and the sites of internal C, NS4A, and NS3 [1,2]. Studies have demonstrated that JEV protease activity mainly depends on the association between NS3 and its co-factor NS2B and that these two-component NS2B-NS3 proteases expressed in *E. coli* are folded correctly with effective proteolytic activity [28,40].

We found that GI-SH7 exhibits eight critical conserved substitutions in the NS2B(H)-NS3(pro) protease region compared to GIII-SH15. Data obtained after the alignment of fifty represented strains of GI and GIII revealed that two mutations in the NS2B hydrophilic domain have a conservation rate of 90–100%, whereas five mutations in NS3 proteases are conserved with a rate of 90–100% and one with a conservation rate of 50–89% [39]. Some previous observations have suggested that differences in the conformational space between NS2B-NS3 proteases of different flaviviruses might lead to differences in substrate recognition and affinity [42–47]. To analyze and compare the cleavage pattern of GI-SH7 with GIII-SH15 NS2B/NS3 proteases, the active and inactivated GI-SH7 and GIII-Sh15 [41] NS2B(H)-NS3(pro) proteases were structured and engineered into PET-Duet 1 vectors for expression in *E. coli* and the cleavage pattern was assessed by Western blot using respective antibodies. Our results demonstrated that GI-SH7 proteases were able to cleave the sites at the internal C, NS2A/NS2B, NS2B/NS3, and NS3/NS4A junctions and exhibited the

same cleavage pattern as previously found for SH-GIII proteases [41], suggesting that viral protease substitution and differential protein conformation do not interfere with the selection of cleavage sites for proteolytic processing and possibly play no role in genotype displacement on this specific side. The identical cleavage patterns of both genotypes comprising critical mutations were supported by previous studies demonstrating that the substrate-recognizing sequence is highly conserved among all flaviviruses and contains two basic residues in P2 and P1 followed by a small unbranched amino acid in P1′ [48,49].

To analyze and compare the proteolytic processing activities of GI-SH7 and GIII-SH15 NS2B/NS3 proteases, the active and inactivated NS2B(H)-NS3(pro) proteases were structured and engineered into *p*-TrcHisA vectors for expression in *E. coli*. The SDS-PAGE of purified proteins revealed the presence of three bands at different sizes, indicating autocleavage, and only the intact NS2B(H)-NS3(pro) proteases band for inactivated/dead NS2B/NS3 proteases, confirming its inactivity. Quantification of blots revealed that SH7 was self-cleaved with a rate of 77.5% and SH15 with a rate of 99.1%. Obvious differences in intact anti-His and anti-NS3 expression were also seen between both strains. These results suggested that GIII-SH15 shows a high autocleavage rate of enzymatically active NS2B(H)-NS3(pro) proteases as compared to GI-SH7. The autocleavage abilities of various flavivirus proteases have also been reported in previous studies [40,46,50].

Enzymatic activity of GI-SH7 and GIII-SH15 recombinant NS2B(H)-NS3(pro) proteases was examined and compared by fluorescence obtained after the hydrolysis of fluorogenic peptide substrates containing the sequence identical to the dibasic cleavage sites of NS2A/NS2B and NS2B/NS3 from JEV polyprotein. Data revealed that proteases from GIII-SH15 possess high proteolytic processing activities when compared to GI-SH7 and the artificial fluorogenic peptide containing a cleavage site from NS2B/NS3 is more efficiently cleaved by JEV proteases as compared to site NS2A/NS2B.

The higher thermal stability at elevated temperatures for GI could be a causative factor related to the enhancement in viral replication of GI viruses. Previously, NS2B/NS3 mutations in the Japanese encephalitis virus were found to enhance the infectivity of GI over GIII in amplifying host cells at elevated temperatures [31]. To assess the influence of viral thermal stability on viral NS2B/NS3 proteases' proteolytic activities, the experiment was repeated using elevated temperatures of 41 °C with fluorogenic substrate NS2B/NS3. The trends were identical to experiments performed at 37 °C and indicated that elevated temperatures do not influence the proteolytic processing activities of viral proteases and GIII-SH15 possesses higher proteolytic activities than GI-SH7 at normal and elevated temperatures.

To determine whether amino acid variations in the hydrophilic or protease domain in viral proteases are responsible and involved in increased proteolytic processing of GIII-SH15, the recombinant proteases were generated by exchanging proteins encoding the hydrophilic domain from NS2B and protease domain from NS3 of the respective strains GI-SH7 and GIII-SH15, resulting in GI/NS2B(H)-GIII/NS3(pro) and GIII/NS2B(H)-GI/NS3(pro)). Exchanging the hydrophilic domain of GI NS2B to GIII in GI protease (GIII/NS2B(H)-GI/NS3(pro)) significantly increased its proteolytic processing activities, as compared with its parental GI protease. The activity of recombinant proteases GIII/NS2B(H)-GI/NS3(pro) became almost similar to that of GIII proteases with non-significant differences among them. On the other hand, after exchanging the hydrophilic domain of GIII NS2B to GI in GIII proteases (GI/NS2B(H)-GIII/NS3(pro)), a significant decrease in its activity was observed, compared to its parental GIII proteases. However, the levels of GI/NS2B(H)-GIII/NS3(pro) protease activity became significantly lower than those of GI protease. Collectively, these results demonstrated that the hydrophilic domain of NS2B determined the difference in NS2B(H)-NS3(pro) protease activities between GI and GIII, suggesting that the mutations in the hydrophilic domain of NS2B may be responsible for the difference in NS2B(H)-NS3(pro) protease activities between GI and GIII.

The NS2B(H) hydrophilic domain possesses two conserved variations at positions 55 (NS2B-D55E) and 65 (NS2B-E65D) in NS2B protein [39]. To determine the contribution of

NS2B-D55E to differential proteolytic processing activities between GI and GIII, we replaced aspartic acid (D) at position 55 of GI proteases with glutamic acid (E) to generate a mutant protease of GI NS2B(H)/D55E-NS3(pro) and substituted aspartic acid (D) for glutamic acid (E) at position 55 of GIII proteases to generate a mutant protease of GIII NS2B(H)/E55D-NS3(pro). NS2B-D55E and NS2B-E55D variation resulted in a conformational change in NS2B(H), as compared with their respective parent strains. Exchanging the amino acid residue at 55 in GI NS2B(H) significantly increased the proteolytic processing activities of GI NS2B(H)/D55E-NS3(pro), as compared to its parental GI protease. However, the levels of GI NS2B(H)/D55E-NS3(pro) protease activities remained lower than those of GIII, indicating the contribution of NS2B-D55E to increase proteolytic processing. When the amino acid at position 55 in GIII NS2B(H) was exchanged from glutamic acid to aspartic acid, the levels of GIII NS2B(H)/E55D-NS3(pro) protease activities significantly decreased, as compared to its parental GIII protease but remained higher than those of GI protease. Collectively, these results demonstrated that the NS2B-D55E variation in the hydrophilic domain of NS2B contributes to the difference in NS2B(H)-NS3(pro) protease activities between GI and GIII. To determine the contribution of NS2B-E65D variation to differential proteolytic processing activities between GI and GIII, we replaced glutamic acid (E) at position 65 of GI protease with aspartic acid (D) to generate a mutant protease of GI NS2B(H)/E65D-NS3(pro) and substituted glutamic acid (E) for aspartic acid (D) at position 65 of GIII proteases to generate a mutant protease of GIII NS2B(H)/D65E-NS3(pro). Substitution of NS2B-E65D NS2B-D65E variations resulted in a conformational change in NS2B(H), as compared with their respective parent strains. Exchanging the amino acid residue at 65 in GI NS2B(H) significantly increased the proteolytic processing activities of GI NS2B(H)/E65D-NS3(pro), as compared to its parental GI protease (Figure 8C). However, the levels of GI NS2B(H)/E65D-NS3(pro) protease activities remained lower than those of GIII protease (Figure 8D), indicating the contribution of NS2B-D55E to increase proteolytic processing. When the amino acid residue at position 65 in GIII NS2B(H) was exchanged, the levels of GIII NS2B(H)/D65E-NS3(pro) protease activities significantly decreased, as compared to its parental GIII proteases, but remained higher than those of GI proteases. These results demonstrated that the NS2B-E65D variation in the hydrophilic domain of NS2B contributed to the difference in NS2B(H)-NS3(pro) protease activities between GI and GIII. However, the six mutations in the NS3(pro) region may also play a role in this differential NS2B/NS3 protease activity. The role of each mutation in the NS3(pro) should also be explored individually or in different combinations in subsequent experiments. Furthermore, additional studies on the structural basis of JEV NS2B-NS3 proteins should be conducted to elucidate conformational changes caused by these variants in detail.

Collectively, these findings indicated that both conserved mutations at positions 55 and 65 in the hydrophilic domain of NS2B contribute individually and together to the increased proteolytic processing activities of GIII proteases over GI in the fluorogenic peptide model. These results are braced by previous findings that demonstrate that NS3 protease activity critically depends on or is controlled by a small NS2B co-factor protein [51,52] and that the presence of a small activating protein or co-factor is a prerequisite for the optimal catalytical activity of flavivirus proteases with natural polyprotein substrates [24,53]. Furthermore, numerous studies have investigated the multifaceted functionality of flavivirus NS2B-NS3 proteases. Replacing or exchanging the acidic residues within the NS2B region of flaviviruses NS2B-NS3 proteases with other acidic residues could impact various elements of protease functioning. Firstly, the substitution of acidic amino acids with different side-chain lengths in NS2B likely influences the structural dynamics of the NS2B-NS3 protease complex. Short or long acidic chains might shift the NS2B positioning relative to NS3, altering its spatial and electrostatic interactions, which could be critical for substrate binding and cleavage. This structural change may alter the enzyme activities by enhancing or hindering its ability to precisely align substrate at the active site [26,54]. Furthermore, as elucidated by Li et al. (2015) [55] and Yildiz et al., 2013 [56], a modification may occur in the active site configuration that impacts substrate binding and catalysis by changing

electrostatic interactions. Secondly, there may be an impact on the protease structure and stability, which is crucial for proper folding and activity. This could lead to protein misfolding or instability [49,57]. Thirdly, the catalytic mechanism could be changed due to altered pKa values or the availability of acidic residues contributing to catalysis. Finally, substrate specificity could be impacted, which may lead to the recognition of alternative substrates or the cleavage of distinct peptide bonds [58,59]. However, extensive structural studies and further experimental verification are essential to validate these impacts. Moreover, studying JEV NS2B-NS3 proteases in the context of glycosylation can also be crucial for understanding their role in antigenicity, infectivity, replication, pathogenesis, immune escape, evolution, and developing vaccines and antiviral therapies [60–62]. Summarizing, our findings demonstrated that the mutations in the hydrophilic domain of NS2B may be involved in the replication advantage of GI over GIII and can provide new insights into the molecular basis of JEV genotype shift. However, further investigations are required to completely comprehend the effect of these variations/mutations in JEV NS2B-NS3 protease activities and viral pathogenesis using other in vitro or/and in vivo models.

4. Material and Methods

4.1. Virus Stock, Cells, and Antibodies

Japanese encephalitis virus GI strain SH7 (MH753129) and GIII strain SH15 (MH753130), isolated from *Cx. tritaeniorhynchus* and *An. sinensis* (respectively) in 2016, were used in this study [21,63]. All JEV strains were plaque-purified three times and amplified in BHK cells at 0.1 MOI as described previously [63]. The fifty percent tissue culture infective dose (TCID50) was determined, and fresh virus suspensions were used in all experiments. Baby hamster kidney cells' (BHK-21) cell line was obtained from the American Type Culture Collection (ATCC) and cultured in Dulbecco's modified Eagle's medium (DMEM, Invitrogen, GIBCO, Carlsbad, CA, USA) containing 10% fetal bovine serum (FBS) (Gibco, Thermo Fisher Scientific, Waltham, MA, USA) and 100 µg/mL streptomycin and 100 IU/mL penicillin at 37 °C. The commercial antibodies used in this study included a GFP (D5.1) XP Rabbit monoclonal antibody (Cell Signaling Technology, Danvers, MA, USA), GAPDH (glyceraldehyde-3-phosphate dehydrogenase) monoclonal antibody (Proteintech, Chicago, IL, USA), monoclonal His-tag antibody (GeneScript, Piscataway, NJ, USA), and a self-generated antibody specific to JEV NS3 [64].

4.2. Sequence Alignment

Amino acid sequences of Japanese encephalitis virus genotypes including GI-SH7 strain (GenBank no MH753129.1) and GIII-SH15 strain (GenBank no MH753130.1) were assembled from the NCBI database (http://www.ncbi.nlm.nih.gov; accessed multiple times between 2019 to 2024). Sequences of recombinant NS2B(H)-NS3(pro) proteases and the predicted/anticipated cleavage sites at internal capsid (internal C), Cap/prM, prM/E, E/NS1, NS1/NS2A, NS2A/NS2B, NS2B/NS3, internal NS3, NS3/NS4A, internal NS4A), NS4A/NS4B, and NS4B/NS5 intersections were aligned using SnapGene (GSL Biotech LLC, San Diego, CA, USA) and MegAlign 7 (DNASTAR Inc., Madison, WI, USA) software.

4.3. Construction of PTrcHis-A NS2B(H)-NS3pro

Total RNAs from BHK cells infected with JEV GI-SH 7 and JEV GIII-SH15 strains were extracted using TRIzol reagent (Thermo Fisher Scientific, Waltham, MA, USA) according to the manufacturer's protocol. Reverse transcription was performed to make cDNA using a PrimeScript RT reagent kit with gDNA Eraser (TaKaRa, Kyoto, Japan). Sequences encoding the C-terminal portion (amino acid 45 to 131) of NS2B and the N-terminal portion (amino acid 1 to 185) of NS3 were amplified and inserted into the multiple cloning site of protein expression plasmid pTrcHisA (Thermo Fisher Scientific, MA, USA) through restriction sites XhoI and EcoRI. The sequence encoding the 96–120 NS2B residues was removed from recombinant pTrcHisA plasmid by PCR-based site-directed mutagenesis [65] using Pfu Ultra II fusion HS DNA polymerase (Agilent, Santa Clara, CA, USA) to generate recombinant

plasmids expressing N-terminal hexahistidine tag fused active NS2B(H)-NS3(pro) proteases [40,52]. The active recombinant NS2B(H)-NS3(pro) proteases were inactivated [50] by replacing a serine at residue 135 with an alanine residue. Point mutations in NS2B(H) regions of proteases were attained through PCR-based site-directed mutagenesis [65]. The resulting constructs were sequenced in both directions through plasmid universal primers (PTrcHis Forward/Reverse) with an ABI Prism 3730 DNA sequencer (Applied Biosystem, Foster City, CA, USA) at Invitrogen (Guangzhou, China).

4.4. Construction of Recombinant PET Duet1 Co-Expressing Artificial GFP Substrate and NS2B(H)-NS3(pro)

Sequences encoding JEV GI (SH 7) active and inactive NS2B(H)-NS3 pro proteases were generated as described previously and cloned into the MCS1 (multiple cloning site 1) of dual protein expression plasmid pETDuet-1 (Novagen, Beijing, China) through restriction sites EcoRI and NotI. For artificial GFP substrate, sequences encoding the anticipated cleavage sites, i.e., internal C, C/prM, prM/E, E/NS1, NS1/NS2A, NS2A/NS2B, NS2B/NS3, internal NS3, NS3/NS4A, internal NS4A, NS4A/NS4B, and NS4B/NS5 intersections, were cloned from JEV GI SH7 (Figure 1B,C) strain with particularly designed oligo dT primer pairs (Shanghai Sunny Biotec, Shanghai, China) by reverse transcriptase polymerase chain reaction (RT-PCR) and inserted between the N-terminal (amino acid 1 to 173) and C-Terminal (amino acid 174 to 239) of GFP by overlap extension PCR. The obtained sequence was cloned to MCS2 (multiple cloning site 2) of pETDuet-1 using [41]. The sequence of twenty alanine residues was inserted between the N-terminal and C-terminal part of GFP to generate a control artificial GFP substrate.

4.5. Detection of Cleavage Sites in Competent E. coli

E. coli BL21 (DE-3) cells were transformed with recombinant pETDuet-1 expressing JEV GI NS2B(H)-NS3(pro) proteases and artificial GFP substrate and incubated at 37 °C until OD600 reached 0.6. Isopropyl b-D-1pthiogalactopyranoside (IPTG) was used to induce expression at a final concentration of 0.70 mM. The cells were harvested after 24 h incubation by centrifugation at $10,000 \times g$ for 10 min at 4 °C. The pellets were washed and resuspended in cold phosphate-buffered saline (PBS 1X) and recentrifuged at $10,000 \times g$ for 10 min at 4 °C. The pellet was subjected to Western blot analysis using specific antibodies as described previously [66]. The cleavage of artificial GFP substrate was detected by monoclonal anti-GFP antibody (GFP (D5.1) XP Rabbit). The expression of NS2B(H)-NS3(pro) was probed by antibodies specific to NS3 [64].

4.6. Expression and Purification of NS2B(H)-NS3(pro) Proteases

PTrc His-A vectors harboring various JEV NS2B-NS3 proteases were propagated in *Escherichia coli* DH5 (TIANGEN Biotech, Beijing, China) and extracted using Plasmid Miniprep Kit (Corning, NY, USA). Extracted constructs were transformed to *E. coli* BL-21 (DE-3) cells for expression and cells were grown in 1000 mL LB medium comprising 100 mg/mL ampicillin at 37 °C until the OD600 reached 0.6. The temperature was reduced to 18 °C and isopropyl b-D-1pthiogalactopyranoside (IPTG) was used to induce expression at a final concentration of 0.70 mM. The cells were incubated for 14 h at 18 °C. The cells were harvested by centrifugation at $8000 \times g$ for 10 min at 4 °C. The pellets were washed and resuspended in cold phosphate-buffered saline (PBS 1X) and recentrifuged at $8000 \times g$ for 10 min at 4 °C. The pellet was kept on ice and resuspended in 40 mL lysis buffer (0.1 M Tris-HCl, 0.3 M NaCl, PH 7.5, 10 mg mL^{-1} DNase, 0.25 mg mL^{-1} lysozyme, and 5 mM MgCl$_2$). Cells were kept at room temperature for 30 min and lysed on ice by sonication with an Ultrasonic Processor XL (Misonix Inc., Farmingdale, NY, USA). Residues in solution were pelleted by centrifugation at $12,000 \times g$ for 30 min at 4 °C and the soluble fraction was filtered through 0.22-micron filters (Merck Millipore Ltd., Cork, Ireland). The supernatant was loaded onto a 5 mL Nickel-Sepharose HisTrap Chelating column (GE Healthcare, Uppsala, Sweden) pre-equilibrated with lysis buffer at a flow rate of 1.0 mL per

minute. The column was washed with five-column volumes of buffer A (0.1 M Tris HCl, pH 7.5, 0.3 M NaCl, 20 mM imidazole) and five-column volumes of buffer B (A (0.1 M Tris HCl, pH 7.5, 0.3 M NaCl, 50 mM imidazole), respectively. Proteins were eluted with ten-column volumes of elution buffer (0.1 M Tris HCl, pH 7.5, 0.3 M NaCl, 250 mM imidazole) in fractions of 1.0 mL in DNA/protease-free Eppendorf tubes. Aliquots of 20 μL from each tube were subjected to 15% SDS-page and gels were stained with One-Step Blue, Protein Gel Stain, 1X (Biotium, Fremont, CA, USA) as per manufacturer instructions. Fractions containing NS2B/NS3 proteins were pooled and desalted through stepwise dialysis as described previously [40]. Purified NS2B-NS3 pro was concentrated to 1.0 mg mL^{-1} using centrifugal filter columns (Centricon 20 mL, 3000 MWCO, Millipore, Burlington, MA, USA). Protein concentration was determined with an enhanced BCA protein assay kit (Beyotime, Shanghai, China) with bovine serum albumin as standard. Samples were stored in 50 mM Tris-HCl, pH 9.0, glycerol (50% v/v) at -20 °C. Proteins were subjected to Western blot analysis using anti-NS3 and His-tagged antibodies.

4.7. Protease Activity Assay

The assay of protease activity of purified NS2B(H)-NS3(pro) was carried out using previously reported fluorogenic peptides from JEV-conserved cleavage sites NS2B/NS3 (Pyr-RTKR-AMC) and NS2A/NS2B (Dabcyl-PNKKRGWP-(EDANS)G) synthesized by A + Peptide (Pudong, Shanghai, China) [40]. Assays were conducted on 96-well black, flat-bottom, tissue culture-treated polystyrene microplates (Corning Life Sciences, MA, USA) in total reaction volume of 0.1 mL containing 0.5 μM NS2B(H)-NS3(pro) proteases, assay buffer (50 mM Tris HCl, pH9.5, 20% glycerol), and fixed amount (10 μL of 100 μmol/L) of fluorescent substrate.

Fluorescence measurements were recorded at zero, 20, 40 min, and after every 40 min interval until 520 min through a multimode plate reader (Bio Tek, Agilent Technologies, Santa Clara, CA, USA) at an excitation wavelength (λ_{ex}) of 360 nm and emission wavelength (λ_{em}) of 460 nm. The assay was carried out with three repeats for each group in two independent experiments at a constant temperature of 37 °C. The inner filter effects of the microplate reader were corrected as described in the literature [67]. The obtained fluorescence data were directly plotted as relative fluorescence units (RFUs) and each time point was individually/singularly analyzed by GraphPad Prism version 7.00 for Windows (GraphPad Software, La Jolla, CA, USA) [50,68]. No significant hydrolysis of peptide substrate was noted in dead NS2B(H)-NS3(pro) and/or groups without enzymes.

4.8. Homology Modeling

The precise structure of JEV NS2B/NS3 proteins has not been thoroughly studied up until now. Thus, in this study, the homologous modeling of GI and GIII virus NS2B/NS3 proteins was carried out with SWISS-MODEL (www.swissmodel.expacy.org; accessed multiple times between 2019 to 2024) by utilizing the template structure of Murray Valley encephalitis virus (MVEV) NS2B/NS3 proteins (PDB: 2WV9). The analysis of protein structure was performed by software pyMOL version 2.4 (http://pymol.org) and SPDV (DeepView 4.1) software (https://spdv.vital-it.ch) [69].

4.9. Statistical Analysis

Statistical analysis was performed using GraphPad Prism version 10 (GraphPad Software, La Jolla, CA, USA). Data were assembled as mean with standard deviation. Significant differences between groups were determined at individual/singular time points using the unpaired (non-parametric) Mann–Whitney test. A "*p*-value" less than 0.05 ($p < 0.05$) was considered as significant.

5. Conclusions

In conclusion, this study uncovers critical insights into the phenomena of Japanese encephalitis virus genotype shifts by identifying and analyzing the specific mutations

within the viral NS2B/NS3 proteases. We have revealed genetic determinants in the hydrophilic domain of NS2B/NS3 proteases, which may play a pivotal role in genotype shifts and viral replication using an artificial fluorogenic peptide model. Importantly, our research has revealed significant differences in protease activities between JEV GI and GIII linked to these mutations, underscoring their functional importance. However, it is crucial to acknowledge that while our study provides essential groundwork, further investigations of observed variations in NS2B/NS3 protease activities using in vivo and other in vitro models are important. Exploring these mutations in different animal models, mosquito vectors, or cellular models will provide a deeper understanding of their biological implications and contribute vital data for understanding the viral replication, pathogenesis, and development of targeted therapies. This research marks a significant enhancement in the understanding of JEV genotype shift, emphasizing the need for continued research attempts, and enhancing our capacity to combat the varied and dynamic nature of the Japanese encephalitis virus and related flaviviruses.

Supplementary Materials: The following supporting information can be downloaded at: https://www.mdpi.com/article/10.3390/ijms252312680/s1.

Institutional Review Board Statement: Not applicable.

Informed Consent Statement: Not applicable.

Data Availability Statement: Relevant data are included within the manuscript.

Conflicts of Interest: The authors declare no conflicts of interest.

References

1. Brecher, M.; Li, Z.; Liu, B.; Zhang, J.; Koetzner, C.A.; Alifarag, A.; Jones, S.A.; Lin, Q.; Kramer, L.D.; Li, H. A conformational switch high-throughput screening assay and allosteric inhibition of the flavivirus NS2B-NS3 protease. *PLoS Pathog.* **2017**, *13*, e1006411. [CrossRef] [PubMed]
2. Rice, C.M.; Lenches, E.M.; Eddy, S.R.; Shin, S.J.; Sheets, R.L.; Strauss, J.H. Nucleotide sequence of yellow fever virus: Implications for flavivirus gene expression and evolution. *Science* **1985**, *229*, 726–733. [CrossRef] [PubMed]
3. Wahaab, A.; Mustafa, B.E.; Hameed, M.; Stevenson, N.J.; Anwar, M.N.; Liu, K.; Wei, J.; Qiu, Y.; Ma, Z. Potential Role of Flavivirus NS2B-NS3 Proteases in Viral Pathogenesis and Anti-flavivirus Drug Discovery Employing Animal Cells and Models: A Review. *Viruses* **2021**, *14*, 44. [CrossRef] [PubMed]
4. Mackenzie, J.; Barrett, A.; Deubel, V. The Japanese encephalitis serological group of flaviviruses: A brief introduction to the group. *Curr. Top. Microbiol. Immunol.* **2002**, *267*, 1–10. [PubMed]
5. Solomon, T.; Vaughn, D. Pathogenesis and clinical features of Japanese encephalitis and West Nile virus infections. *Curr. Top. Microbiol. Immunol.* **2002**, *267*, 171–194.
6. Johari, J.; Kianmehr, A.; Mustafa, M.R.; Abubakar, S.; Zandi, K. Antiviral activity of baicalein and quercetin against the Japanese encephalitis virus. *Int. J. Mol. Sci.* **2012**, *13*, 16785–16795. [CrossRef]

7. Campbell, G.L.; Hills, S.L.; Fischer, M.; Jacobson, J.A.; Hoke, C.H.; Hombach, J.M.; Marfin, A.A.; Solomon, T.; Tsai, T.F.; Tsu, V.D.; et al. Estimated global incidence of Japanese encephalitis: A systematic review. *Bull. World Health Organ.* **2011**, *89*, 766–774, 774a–774e. [CrossRef]

8. Sarkar, A.; Taraphdar, D.; Mukhopadhyay, S.K.; Chakrabarti, S.; Chatterjee, S. Molecular evidence for the occurrence of Japanese encephalitis virus genotype I and III infection associated with acute encephalitis in patients of West Bengal, India, 2010. *Virol. J.* **2012**, *9*, 271. [CrossRef]

9. Huang, J.H.; Lin, T.H.; Teng, H.J.; Su, C.L.; Tsai, K.H.; Lu, L.C.; Lin, C.; Yang, C.F.; Chang, S.F.; Liao, T.L.; et al. Molecular epidemiology of Japanese encephalitis virus, Taiwan. *Emerg. Infect. Dis.* **2010**, *16*, 876–878. [CrossRef]

10. Nitatpattana, N.; Dubot-Pérès, A.; Gouilh, M.A.; Souris, M.; Barbazan, P.; Yoksan, S.; de Lamballerie, X.; Gonzalez, J.P. Change in Japanese encephalitis virus distribution, Thailand. *Emerg. Infect. Dis.* **2008**, *14*, 1762–1765. [CrossRef]

11. Pan, X.L.; Liu, H.; Wang, H.Y.; Fu, S.H.; Liu, H.Z.; Zhang, H.L.; Li, M.H.; Gao, X.Y.; Wang, J.L.; Sun, X.H.; et al. Emergence of genotype I of Japanese encephalitis virus as the dominant genotype in Asia. *J. Virol.* **2011**, *85*, 9847–9853. [CrossRef] [PubMed]

12. Ma, S.-P.; Yoshida, Y.; Makino, Y.; Tadano, M.; Ono, T.; Ogawa, M. Short report: A major genotype of japanese encephalitis virus currently circulating in Japan. *Am. J. Trop. Med. Hyg.* **2003**, *69*, 151–154. [CrossRef] [PubMed]

13. Nga, P.T.; Parquet, M.D.C.; Cuong, V.D.; Ma, S.P.; Hasebe, F.; Inoue, S.; Makino, Y.; Takagi, M.; Nam, V.S.; Morita, K. Shift in Japanese encephalitis virus (JEV) genotype circulating in northern Vietnam: Implications for frequent introductions of JEV from Southeast Asia to East Asia. *J. Gen. Virol.* **2004**, *85 Pt 6*, 1625–1631. [CrossRef]

14. Hameed, M.; Wahaab, A.; Shan, T.; Wang, X.; Khan, S.; Di, D.; Xiqian, L.; Zhang, J.-J.; Anwar, M.N.; Nawaz, M.; et al. A Metagenomic Analysis of Mosquito Virome Collected From Different Animal Farms at Yunnan–Myanmar Border of China. *Front. Microbiol.* **2021**, *11*, 3601. [CrossRef] [PubMed]

15. Schuh, A.J.; Ward, M.J.; Brown, A.J.; Barrett, A.D. Phylogeography of Japanese encephalitis virus: Genotype is associated with climate. *PLoS Neglected Trop. Dis.* **2013**, *7*, e2411. [CrossRef] [PubMed]

16. Do, L.P.; Bui, T.M.; Phan, N.T. Mechanism of Japanese encephalitis virus genotypes replacement based on human, porcine and mosquito-originated cell lines model. *Asian Pac. J. Trop. Med.* **2016**, *9*, 333–336. [CrossRef] [PubMed]

17. Schuh, A.J.; Ward, M.J.; Leigh Brown, A.J.; Barrett, A.D. Dynamics of the emergence and establishment of a newly dominant genotype of Japanese encephalitis virus throughout Asia. *J. Virol.* **2014**, *88*, 4522–4532. [CrossRef] [PubMed]

18. Nemeth, N.; Bosco-Lauth, A.; Oesterle, P.; Kohler, D.; Bowen, R. North American birds as potential amplifying hosts of Japanese encephalitis virus. *Am. J. Trop. Med. Hyg.* **2012**, *87*, 760–767. [CrossRef] [PubMed]

19. Hameed, M.; Wahaab, A.; Nawaz, M.; Khan, S.; Nazir, J.; Liu, K.; Wei, J.; Ma, Z. Potential Role of Birds in Japanese Encephalitis Virus Zoonotic Transmission and Genotype Shift. *Viruses* **2021**, *13*, 357. [CrossRef]

20. Xiao, C.; Li, C.; Di, D.; Cappelle, J.; Liu, L.; Wang, X.; Pang, L.; Xu, J.; Liu, K.; Li, B.; et al. Differential replication efficiencies between Japanese encephalitis virus genotype I and III in avian cultured cells and young domestic ducklings. *PLoS Neglected Trop. Dis.* **2018**, *12*, e0007046. [CrossRef]

21. Hameed, M.; Liu, K.; Anwar, M.N.; Wahaab, A.; Safdar, A.; Di, D.; Boruah, P.; Xu, J.; Wang, X.; Li, B.; et al. The emerged genotype I of Japanese encephalitis virus shows an infectivity similar to genotype III in Culex pipiens mosquitoes from China. *PLoS Neglected Trop. Dis.* **2019**, *13*, e0007716. [CrossRef] [PubMed]

22. Han, N.; Adams, J.; Chen, P.; Guo, Z.Y.; Zhong, X.F.; Fang, W.; Li, N.; Wen, L.; Tao, X.Y.; Yuan, Z.M.; et al. Comparison of genotypes I and III in Japanese encephalitis virus reveals distinct differences in their genetic and host diversity. *J. Virol.* **2014**, *88*, 11469–11479. [CrossRef] [PubMed]

23. Huang, Q.; Chen, A.S.; Li, Q.; Kang, C. Expression, purification, and initial structural characterization of nonstructural protein 2B, an integral membrane protein of Dengue-2 virus, in detergent micelles. *Protein Expr. Purif.* **2011**, *80*, 169–175. [CrossRef] [PubMed]

24. Chambers, T.J.; Grakoui, A.; Rice, C.M. Processing of the yellow fever virus nonstructural polyprotein: A catalytically active NS3 proteinase domain and NS2B are required for cleavages at dibasic sites. *J. Virol.* **1991**, *65*, 6042–6050. [CrossRef] [PubMed]

25. Aleshin, A.E.; Shiryaev, S.A.; Strongin, A.Y.; Liddington, R.C. Structural evidence for regulation and specificity of flaviviral proteases and evolution of the Flaviviridae fold. *Protein Sci. A Publ. Protein Soc.* **2007**, *16*, 795–806. [CrossRef]

26. Erbel, P.; Schiering, N.; D'Arcy, A.; Renatus, M.; Kroemer, M.; Lim, S.P.; Yin, Z.; Keller, T.H.; Vasudevan, S.G.; Hommel, U. Structural basis for the activation of flaviviral NS3 proteases from dengue and West Nile virus. *Nat. Struct. Mol. Biol.* **2006**, *13*, 372–373. [CrossRef]

27. Hill, M.E.; Kumar, A.; Wells, J.A.; Hobman, T.C.; Julien, O.; Hardy, J.A. The Unique Cofactor Region of Zika Virus NS2B–NS3 Protease Facilitates Cleavage of Key Host Proteins. *ACS Chem. Biol.* **2018**, *13*, 2398–2405. [CrossRef]

28. Brand, C.; Bisaillon, M.; Geiss, B.J. Organization of the Flavivirus RNA replicase complex. *Wiley Interdiscip. Rev. RNA* **2017**, *8*, e1437. [CrossRef]

29. Kim, S.B.; Umezawa, Y.; Kanno, K.A.; Tao, H. An Integrated-Molecule-Format Multicolor Probe for Monitoring Multiple Activities of a Bioactive Small Molecule. *ACS Chem. Biol.* **2008**, *3*, 359–372. [CrossRef]

30. Azad, T.; Tashakor, A.; Hosseinkhani, S. Split-luciferase complementary assay: Applications, recent developments, and future perspectives. *Anal. Bioanal. Chem.* **2014**, *406*, 5541–5560. [CrossRef]

31. Fan, Y.C.; Liang, J.J.; Chen, J.M.; Lin, J.W.; Chen, Y.Y.; Su, K.H.; Lin, C.C.; Tu, W.C.; Chiou, M.T.; Ou, S.C.; et al. NS2B/NS3 mutations enhance the infectivity of genotype I Japanese encephalitis virus in amplifying hosts. *PLoS Pathog.* **2019**, *15*, e1007992. [CrossRef] [PubMed]

32. Kao, Y.T.; Lai, M.M.C.; Yu, C.Y. How Dengue Virus Circumvents Innate Immunity. *Front. Immunol.* **2018**, *9*, 2860. [CrossRef] [PubMed]

33. Liang, J.J.; Liao, C.L.; Liao, J.T.; Lee, Y.L.; Lin, Y.L. A Japanese encephalitis virus vaccine candidate strain is attenuated by decreasing its interferon antagonistic ability. *Vaccine* **2009**, *27*, 2746–2754. [CrossRef] [PubMed]

34. Ding, Q.; Gaska, J.M.; Douam, F.; Wei, L.; Kim, D.; Balev, M.; Heller, B.; Ploss, A. Species-specific disruption of STING-dependent antiviral cellular defenses by the Zika virus NS2B3 protease. *Proc. Natl. Acad. Sci. USA* **2018**, *115*, E6310–E6318. [CrossRef] [PubMed]

35. Wang, Z.Y.; Zhen, Z.D.; Fan, D.Y.; Qin, C.F.; Han, D.S.; Zhou, H.N.; Wang, P.G.; An, J. Axl Deficiency Promotes the Neuroinvasion of Japanese Encephalitis Virus by Enhancing IL-1α Production from Pyroptotic Macrophages. *J. Virol.* **2020**, *94*, 17. [CrossRef]

36. Xie, S.; Liang, Z.; Yang, X.; Pan, J.; Yu, D.; Li, T.; Cao, R. Japanese Encephalitis Virus NS2B-3 Protein Complex Promotes Cell Apoptosis and Viral Particle Release by Down-Regulating the Expression of AXL. *Virol. Sin.* **2021**, *36*, 1503–1519. [CrossRef]

37. Bhimaneni, S.; Kumar, A. Abscisic acid and aloe-emodin against NS2B-NS3A protease of Japanese encephalitis virus. *Environ. Sci. Pollut. Res. Int.* **2022**, *29*, 8759–8766. [CrossRef]

38. Navyashree, V.; Kant, K.; Kumar, A. Natural chemical entities from Arisaema genus might be a promising break-through against Japanese encephalitis virus infection: A molecular docking and dynamics approach. *J. Biomol. Struct. Dyn.* **2021**, *39*, 1404–1416. [CrossRef]

39. Li, C.; Di, D.; Huang, H.; Wang, X.; Xia, Q.; Ma, X.; Liu, K.; Li, B.; Shao, D.; Qiu, Y.; et al. NS5-V372A and NS5-H386Y variations are responsible for differences in interferon α/β induction and co-contribute to the replication advantage of Japanese encephalitis virus genotype I over genotype III in ducklings. *PLoS Pathog.* **2020**, *16*, e1008773. [CrossRef]

40. Junaid, M.; Chalayut, C.; Sehgelmeble Torrejon, A.; Angsuthanasombat, C.; Shutava, I.; Lapins, M.; Wikberg, J.E.; Katzenmeier, G. Enzymatic analysis of recombinant Japanese encephalitis virus NS2B(H)-NS3pro protease with fluorogenic model peptide substrates. *PLoS ONE* **2012**, *7*, e36872. [CrossRef]

41. Wahaab, A.; Liu, K.; Hameed, M.; Anwar, M.N.; Kang, L.; Li, C.; Ma, X.; Wajid, A.; Yang, Y.; Khan, U.H.; et al. Identification of Cleavage Sites Proteolytically Processed by NS2B-NS3 Protease in Polyprotein of Japanese Encephalitis Virus. *Pathogens* **2021**, *10*, 102. [CrossRef] [PubMed]

42. Niyomrattanakit, P.; Winoyanuwattikun, P.; Chanprapaph, S.; Angsuthanasombat, C.; Panyim, S.; Katzenmeier, G. Identification of residues in the dengue virus type 2 NS2B cofactor that are critical for NS3 protease activation. *J. Virol.* **2004**, *78*, 13708–13716. [CrossRef] [PubMed]

43. Chambers, T.J.; Droll, D.A.; Tang, Y.; Liang, Y.; Ganesh, V.K.; Murthy, K.H.M.; Nickells, M. Yellow fever virus NS2B-NS3 protease: Characterization of charged-to-alanine mutant and revertant viruses and analysis of polyprotein-cleavage activities. *J. Gen. Virol.* **2005**, *86 Pt 5*, 1403–1413. [CrossRef] [PubMed]

44. Droll, D.A.; Krishna Murthy, H.M.; Chambers, T.J. Yellow fever virus NS2B-NS3 protease: Charged-to-alanine mutagenesis and deletion analysis define regions important for protease complex formation and function. *Virology* **2000**, *275*, 335–347. [CrossRef] [PubMed]

45. Wu, C.F.; Wang, S.H.; Sun, C.M.; Hu, S.T.; Syu, W.J. Activation of dengue protease autocleavage at the NS2B-NS3 junction by recombinant NS3 and GST-NS2B fusion proteins. *J. Virol. Methods* **2003**, *114*, 45–54. [CrossRef]

46. Lin, C.-W.; Huang, H.-D.; Shiu, S.-Y.; Chen, W.-J.; Tsai, M.-H.; Huang, S.-H.; Wan, L.; Lin, Y.-J. Functional determinants of NS2B for activation of Japanese encephalitis virus NS3 protease. *Virus Res.* **2007**, *127*, 88–94. [CrossRef]

47. Jan, L.R.; Yang, C.S.; Trent, D.W.; Falgout, B.; Lai, C.J. Processing of Japanese encephalitis virus non-structural proteins: NS2B-NS3 complex and heterologous proteases. *J. Gen. Virol.* **1995**, *76 Pt 3*, 573–580. [CrossRef]

48. Niyomrattanakit, P.; Yahorava, S.; Mutule, I.; Mutulis, F.; Petrovska, R.; Prusis, P.; Katzenmeier, G.; Wikberg, J.E. Probing the substrate specificity of the dengue virus type 2 NS3 serine protease by using internally quenched fluorescent peptides. *Biochem. J.* **2006**, *397*, 203–211. [CrossRef]

49. Chappell, K.J.; Stoermer, M.J.; Fairlie, D.P.; Young, P.R. Insights to substrate binding and processing by West Nile Virus NS3 protease through combined modeling, protease mutagenesis, and kinetic studies. *J. Biol. Chem.* **2006**, *281*, 38448–38458. [CrossRef]

50. Bera, A.K.; Kuhn, R.J.; Smith, J.L. Functional characterization of cis and trans activity of the Flavivirus NS2B-NS3 protease. *J. Biol. Chem.* **2007**, *282*, 12883–12892. [CrossRef]

51. Leung, D.; Schroder, K.; White, H.; Fang, N.X.; Stoermer, M.J.; Abbenante, G.; Martin, J.L.; Young, P.R.; Fairlie, D.P. Activity of recombinant dengue 2 virus NS3 protease in the presence of a truncated NS2B co-factor, small peptide substrates, and inhibitors. *J. Biol. Chem.* **2001**, *276*, 45762–45771. [CrossRef] [PubMed]

52. Yusof, R.; Clum, S.; Wetzel, M.; Murthy, H.M.K.; Padmanabhan, R. Purified NS2B/NS3 Serine Protease of Dengue Virus Type 2 Exhibits Cofactor NS2B Dependence for Cleavage of Substrates with Dibasic Amino Acids in Vitro. *J. Biol. Chem.* **2000**, *275*, 9963–9969. [CrossRef] [PubMed]

53. Bartenschlager, R.; Lohmann, V.; Wilkinson, T.; Koch, J.O. Complex formation between the NS3 serine-type proteinase of the hepatitis C virus and NS4A and its importance for polyprotein maturation. *J. Virol.* **1995**, *69*, 7519–7528. [CrossRef] [PubMed]

54. Starvaggi, J.; Previti, S.; Zappalà, M.; Ettari, R. The Inhibition of NS2B/NS3 Protease: A New Therapeutic Opportunity to Treat Dengue and Zika Virus Infection. *Int. J. Mol. Sci.* **2024**, *25*, 4376. [CrossRef] [PubMed]

55. Li, Y.; Li, Q.; Wong, Y.L.; Liew, L.S.Y.; Kang, C. Membrane topology of NS2B of dengue virus revealed by NMR spectroscopy. *Biochim. Biophys. Acta (BBA) Biomembr.* **2015**, *1848 Pt A*, 2244–2252. [CrossRef]

56. Yildiz, M.; Ghosh, S.; Bell, J.A.; Sherman, W.; Hardy, J.A. Allosteric inhibition of the NS2B-NS3 protease from dengue virus. *ACS Chem. Biol.* **2013**, *8*, 2744–2752. [CrossRef]

57. Nitsche, C.; Holloway, S.; Schirmeister, T.; Klein, C.D. Biochemistry and Medicinal Chemistry of the Dengue Virus Protease. *Chem. Rev.* **2014**, *114*, 11348–11381. [CrossRef]

58. Shiryaev, S.A.; Farhy, C.; Pinto, A.; Huang, C.T.; Simonetti, N.; Elong Ngono, A.; Dewing, A.; Shresta, S.; Pinkerton, A.B.; Cieplak, P.; et al. Characterization of the Zika virus two-component NS2B-NS3 protease and structure-assisted identification of allosteric small-molecule antagonists. *Antivir. Res.* **2017**, *143*, 218–229. [CrossRef]

59. Yin, Z.; Patel, S.J.; Wang, W.L.; Wang, G.; Chan, W.L.; Rao, K.R.; Alam, J.; Jeyaraj, D.A.; Ngew, X.; Patel, V.; et al. Peptide inhibitors of Dengue virus NS3 protease. Part 1: Warhead. *Bioorg. Med. Chem. Lett.* **2006**, *16*, 36–39. [CrossRef]

60. Beatty, P.R.; Puerta-Guardo, H.; Killingbeck, S.S.; Glasner, D.R.; Hopkins, K.; Harris, E. Dengue virus NS1 triggers endothelial permeability and vascular leak that is prevented by NS1 vaccination. *Sci. Transl. Med.* **2015**, *7*, 304ra141. [CrossRef]

61. Glasner, D.R.; Puerta-Guardo, H.; Beatty, P.R.; Harris, E. The Good, the Bad, and the Shocking: The Multiple Roles of Dengue Virus Nonstructural Protein 1 in Protection and Pathogenesis. *Annu. Rev. Virol.* **2018**, *5*, 227–253. [CrossRef] [PubMed]

62. Navarro-Sanchez, E.; Altmeyer, R.; Amara, A.; Schwartz, O.; Fieschi, F.; Virelizier, J.L.; Arenzana-Seisdedos, F.; Desprès, P. Dendritic-cell-specific ICAM3-grabbing non-integrin is essential for the productive infection of human dendritic cells by mosquito-cell-derived dengue viruses. *EMBO Rep.* **2003**, *4*, 723–728. [CrossRef] [PubMed]

63. Xiao, C.; Wang, X.; Cui, G.; Pang, L.; Xu, J.; Li, C.; Zhang, J.; Liu, K.; Li, B.; Shao, D.; et al. Possible pathogenicity of Japanese encephalitis virus in newly hatched domestic ducklings. *Vet. Microbiol.* **2018**, *227*, 8–11. [CrossRef] [PubMed]

64. Deng, X.; Shi, Z.; Li, S.; Wang, X.; Qiu, Y.; Shao, D.; Wei, J.; Tong, G.; Ma, Z. Characterization of nonstructural protein 3 of a neurovirulent Japanese encephalitis virus strain isolated from a pig. *Virol. J.* **2011**, *8*, 209. [CrossRef] [PubMed]

65. Li, X.; Qiu, Y.; Shen, Y.; Ding, C.; Liu, P.; Zhou, J.; Ma, Z. Splicing together different regions of a gene by modified polymerase chain reaction-based site-directed mutagenesis. *Anal. Biochem.* **2008**, *373*, 398–400. [CrossRef]

66. Zhu, Z.; Shi, Z.; Yan, W.; Wei, J.; Shao, D.; Deng, X.; Wang, S.; Li, B.; Tong, G.; Ma, Z. Nonstructural protein 1 of influenza A virus interacts with human guanylate-binding protein 1 to antagonize antiviral activity. *PLoS ONE* **2013**, *8*, e55920. [CrossRef]

67. Liu, Y.; Kati, W.; Chen, C.M.; Tripathi, R.; Molla, A.; Kohlbrenner, W. Use of a fluorescence plate reader for measuring kinetic parameters with inner filter effect correction. *Anal. Biochem.* **1999**, *267*, 331–335. [CrossRef]

68. Phoo, W.W.; Li, Y.; Zhang, Z.; Lee, M.Y.; Loh, Y.R.; Tan, Y.B.; Ng, E.Y.; Lescar, J.; Kang, C.; Luo, D. Structure of the NS2B-NS3 protease from Zika virus after self-cleavage. *Nat. Commun.* **2016**, *7*, 13410. [CrossRef]

69. Barber, R.D. Software to Visualize Proteins and Perform Structural Alignments. *Curr. Protoc.* **2021**, *1*, e292. [CrossRef]